SHEAR BEHAVIOR OF HYBRID FIBER REINFORCED CONCRETE (HFRC) BEAMS WITHOUT WEB REINFORCEMENT

by

Adem Afşın Ulu

B.Sc., Civil Engineering, Boğaziçi University, 2007

Submitted to the Institute for Graduate Studies in
Science and Engineering in partial fulfillment of
the requirements for the degree of
Master of Science

Graduate Program in Civil Engineering
Boğaziçi University

2011

ACKNOWLEDGEMENTS

I would like to express my gratitude to all the people who in one way or another contributed to the development of this research. I would like to express my sincere appreciation to my advisor Prof. Dr. Cengiz Karakoç; thank you for your valuable help in instructing, guiding and supporting me throughout the duration of this project.

Also, I would like to special thank my Co-Advisor Assist. Prof. Dr. Nilüfer Özyurt Zihnioğlu for encouraging me to the thesis. I am appreciating members of my Master's thesis examination committee: Prof. Dr. Turan Özturan, Prof. Dr. Alper İlki, and Assist. Prof. Dr. Kutay Orakçal for their knowledgeable and in-depth comments and advice.

I would like to thank to Anıl Niş, Abdullah Akça and İrem Şanal for their help and suggestions. I want to express special thanks to technicians Ümit Melep, Hasan Şenel and Mesut Kardaş for their assistance during the experiments. Contributions of AKÇANSA A.Ş. and Tolga Ilıca are also appreciated.

Finally, I would like to thank my family for their continuous support and encouragement.

ABSTRACT

SHEAR BEHAVIOR OF HYBRID FIBER REINFORCED CONCRETE (HFRC) BEAMS WITHOUT WEB REINFORCEMENT

This study was conducted to investigate the effects of hybrid fiber combinations on shear capacity of large size reinforced concrete beams. Ten hybrid fiber reinforced concrete beams were cast. Fiber volume was varied from 0% to 1.5%. Two fibre types (RC-65/35-BN and RC-80/60-BN) were used for the hybrid combinations. In addition to that, two types of shear span-to-effective depth ratios (a/d) (2 and 3.75) were used. Four-point bending tests were applied to examine shear behavior. Effects of shear span to effective depth ratio, fiber volume, hybrid combination on mechanical performance were discussed. Moreover, results of this study was compared with the results of a previous study (Şen, 2009) in order to observe the differences between hybrid and one type of fiber reinforcement.

The test results showed that all the beams with an a/d ratio of 2 failed under shear compression type of failure. On the other hand, the beams with an a/d of 3.75 failed under diagonal tension type of failure. When results were examined, failure mode was found to not change with increasing fiber volume ratio. Average stresses at first crack formation and at ultimate were found to decrease when shear span-to-effective depth ratio increased. These results were consistent with the results of the previous study (Şen, 2009) and available literature. Shear capacity of the beams were found to increase with increase in fiber volume ratio. The greatest increase was observed when fiber volume ratio was increased from 0.5 to 0.75%. Fiber contribution was found to vary for different failure modes. Fiber contribution was higher when a/d ratio

was small. This is due to different failure modes occurring for different a/d values. When a/d ratio is 2, shear compression failure occurred. In this type of failure, crack was found to open wider before the specimen failed when compared to the diagonal tension failure (observed when a/d is 3.75). Therefore, effect of using fibers was more pronounced when a/d value was 2.0. When the results of this study were compared with the results of a previous study (Şen, 2009), in which similar specimens and testing set-up were used, hybrid combinations were found to be more effective in increasing shear capacity compared to single type of fiber reinforcement. This is explained by more effective crack arresting mechanism in case of hybrid combination. Using two sizes of fibers are useful since different size of cracks were captured and arrested at different meso and macro levels.

ÖZET

GÖVDE DONATISIZ HİBRİT ÇELİK LİF KATKILI BETONARME KİRİŞLERİN KESME DAVRANIŞI

Bu çalışma hibrit liflerin büyük ölçekli kiriş numunelerinin kesme kapasitesine olan etkisini araştırmak amacıyla yapılmıştır. On adet hibrit lif katkılı betonarme kiriş üretilmiştir. Lif oranları 0% ile 1.5% arasında değişmiştir. Hibrit karışım için iki çeşit lif (RC-65/35-BN ve RC-80/60-BN) kullanılmıştır. Buna ek olarak iki çeşit kiriş kesme açıklığının kiriş etkili derinliğine oranı (a/d) (2 ve 3.75) kullanılmıştır. Kesme davranışını incelemek için dört noktasal eğilme deneyi uygulanmıştır. Kiriş kesme açıklığının kiriş etkili derinliğine oranının (a/d), lif miktarı ve hibrit karışımın mekanik performansa etkisi tartışılmıştır. Ek olarak bu çalışmadaki sonuçlar hibrit ve tek tip lif katkılı betonarme kirişlerin performanslarının farkını gözlemlemek için bir önceki yapılan çalışmanın sonuçları (Şen, 2009) ile mukayese edilmiştir.

Test sonuçları a/d oranı 2 olan bütün kirişlerin kesme basıncı altında kırıldığını göstermiştir. Diğer taraftan a/d oranı 3.75 olan kirişler de diagonal gerilme çatlağı altında kırılmışlardır. Sonuçlar incelendiğinde, lif oranına göre kırılma türlerinin değişmediği görülmüştür. Bundan başka ilk çatlak oluşumunda ortalama kesme gerilmesi ve kesme dayanımının a/d oranı arttıkça azaldığı görülmüştür. Bu sonuçlar bir önceki çalışma ve diğer çalışmalar ile uyumludur. Kirişlerin kesme dayanımlarının lif oranı ile arttığı bulunmuştur. En çok artış lif oranı 0.5% den 0.75% ye çıktığında görülmüştür. Lif katkısının farklı kırılma türlerine göre değişiklik gösterdiği belirlenmiştir. Lif katkısının a/d oranı küçük olduğunda daha fazla olduğu görülmüştür. Bu yüzden farklı a/d oranlarında farklı kırılma türleri oluşmuştur. Bu tip kırılmalarda çatlak genişliğinin diagonal çekme kırılma türüne (a/d 3.75'ken gözlemlenmiştir) göre

daha fazla olduğu görülmüştür. Bu yüzden, lif etkisi a/d oranı 2 olduğu zaman daha fazla belirgindir. Bu çalışma ile önceki yapılmış çalışma (Şen, 2009) karşılaştırıldığında aynı numuneler ve test düzeneği kullanılmıştır. Aynı lif oranlarında hibrit lif katkılı numuneler tek tip lifli numunelere göre kesme kapasitesinin artışında daha etkili olduğu görülmüştür. Bu durum hibrit karışımlardaki çatlak önleme mekanizmasının daha etkili olduğu ile açıklanabilir. İki farklı boyutta lif kullanmanın daha yararlı olduğu çünkü farklı boyuttaki çatlakların (orta ve büyük) açılmasının önlendiği sonucuna varılmıştır.

TABLE OF CONTENTS

LIST OF FIGURES

LIST OF TABLES

LIST OF SYMBOLS

a	Shear Span
a/d	Shear span-to-effective depth ratio
b_w	Width of specimen
d	Effective depth of specimen
d_f	Diameter of fiber
f_c	Compressive strength of concrete
f_{ck}	Characteristic compressive Strength of concrete
$f_{t(max)}$	Maximum tensile stress
h	Depth of specimen
l_f	Length of fiber
l_f/d_f	Aspect Ratio
P_{max}	Maximum load
V	Shear force
V_a	Aggregate interlock force
V_c	Shear resistance of concrete
V_{cr}	Cracking shear force
V_{cz}	Shear resistance of the uncracked concrete
V_d	Dowel action
V_f	Volume fraction
$V_{max}/\sqrt{f_c}b_w d$	Normalized shear stress
V_s	Shear reinforcement resistance
V_u	Ultimate shear force at failure
ρ	Longitudinal reinforcement ratio
σ_c	Compressive stress
σ_t	Tensile stress
τ_s	Shear stress

LIST OF ABBREVIATIONS

HSC	High strength concrete
NSC	Normal strength concrete
SCC	Self-Consolidating Concrete

1. INTRODUCTION

It is known that concrete is a brittle material; therefore in reinforced concrete structures, shear concept is an important topic for design of structures. Shear failure of reinforced concrete slender beams without stirrups is typically brittle and sudden. It usually occurs when the principal tensile stress within the shear span exceeds the tensile strength of concrete and a diagonal crack propagates through the beam. In order to prevent shear failure, conventional shear reinforcement in the form of stirrups is commonly used in RC beams.

Apart from the conventional shear reinforcement known as stirrups, discrete steel fibers improve the shear reinforcement of RC beams. Short discrete steel fibers can be used as shear reinforcement. Experimental investigations on reinforced normal strength concrete (FRNSC) beams have shown that the inclusion of uniformly distributed, randomly oriented, short discrete steel fibers in concrete improved the shear resistance owing to an increase in tensile strength, which delays the formation and growth of cracks. Subsequent to cracking, fibers also have the ability to bridge shear cracks, improving the post-cracking behavior, and potentially changing the failure mode from brittle to ductile and thus, the addition of fibers in adequate quantities may be effective at supplementing or replacing conventional shear reinforcement in concrete members (Greenough and Nehdi, 2008).

There are several advantages of using fibers rather than stirrups to resist shear forces in reinforced concrete structures. At first, fibers are randomly distributed throughout the concrete volume at relatively small spacings and thus provide equal resistance to stresses in all directions. This may be especially beneficial in structures design to resist shear forces due to earthquake and wind loading. Secondly, fibers increase the concrete's resistance to crack formation and propagation. Thirdly, the increased resistance of concrete cover to spalling and cracking helps to protect steel from corrosion in harsh environments and, hence, develop structural durability. Another advantage is to profit from high labor costs and construction time. In other words,

fibers reduce the time and labor costs (Imam, 1997).

In fiber reinforced concrete (FRC), some parameters that affect the ultimate shear strength are concrete compressive strength (f_c), shear span-to-effective depth ratio (a/d), longitudinal reinforcement ratio (ρ), aspect ratio (l_f/d_f), shape of the steel fiber and volume ratio (V_f).

In this study, the main purpose is not comparing shear performances of stirrups and fibers in concrete. It is to investigate the influence of hybrid steel fibers on shear strength and to observe shear behavior and failure modes of reinforced concrete beams. In addition to that, relationship between volume fractions and shear strength is investigated and the effect of shear span-to-effective depth ratio on shear strength under four point loading test is examined.

2. LITERATURE REVIEW

2.1. Shear Behavior of Reinforced Concrete Beams

Members of reinforced concrete structures are usually subjected to shear as well as flexure and axial loads. Shear strength of reinforced concrete is quite high. Thus, shear force does not create any serious problems in reinforced concrete members. However, principal tensile stresses caused by shear combined with other stresses create a critical problem for reinforced concrete members due to the low tensile strength of concrete.

When an elementary area is subjected to pure shear, the failure is due to the principal tensile stresses. The elementary area (each dimension is 1 mm) shown in Figure 2.1 is exposed to pure shear and shear stresses on each face are shown. Using the classical formulas for stress transformation or by sketching a Mohr's circle, the principal tensile stress, which occurs on a plane making an angle of 45^0 with the x-axis and principal compressive stress, which occurs on a plane orthogonal to the plane of the principal stress are equal in magnitude to the shear stress (Ersoy, 1994).

This is illustrated in Figure 2.1. Since the two principal stresses and the maximum shear stress are equal, the element will fail in tension, because tensile strength of concrete is lower than its compressive and shear strengths. The failure occurs by formation of a crack orthogonal to the principal tensile stress as shown in Figure 2.1. Since the crack is inclined with respect to the beam axis, such a crack is usually called diagonal tension crack. The principal tensile stresses are usually referred to as diagonal

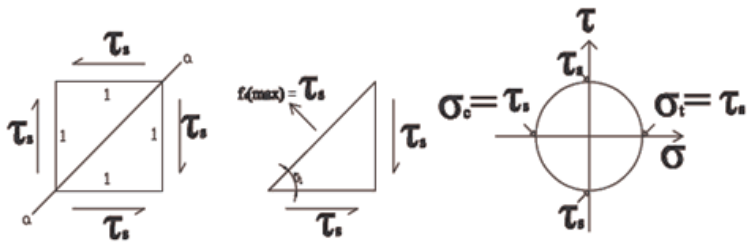

Figure 2.1. Element in pure shear and principal tensile stress.

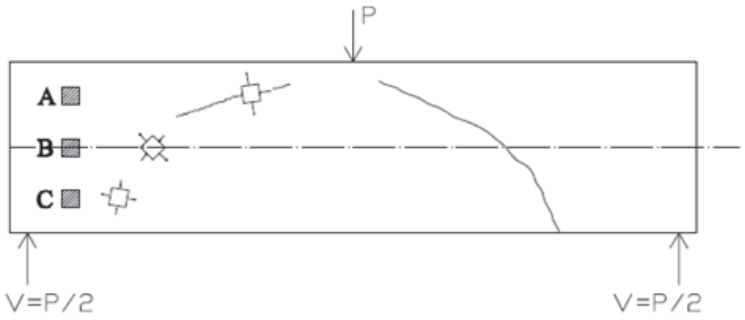

Figure 2.2. The shape or the inclination of the diagonal tension cracks.

tensile stresses (Ersoy, 1994).

Diagonal tension can cause severe diagonal cracking which can bring about failure of the member if necessary precautions are not taken by suitably designed shear reinforcement. Diagonal tension failures are usually very sudden and brittle and therefore such failures should be prevented if a ductile behavior is desired.

The shape or the inclination of the diagonal tension cracks is determined by the orientation of the principal tensile stresses. In Figure 2.2, three elementary areas A, B and C are analyzed, each located at a different level along the beam depth. On this figure, the state of stresses on each elementary area, magnitude and direction of principal tensile stresses are shown. The cracks which form perpendicular to the direction of the principal tensile stresses are also marked on the figure. The direction of the diagonal cracks obtained from these three cases has been used to trace the crack pattern along the beam depth. According to this sketch, the crack is almost perpendicular to the beam axis at the tension face, is almost 45^0 at the level of the neutral axis and is very flat near the compression face. The crack pattern observed in tests is very similar to what has been described. Therefore, it can be concluded that what has been called as shear cracking and shear failure are really caused by principle tensile stresses (Ersoy, 1994).

2.2. Behavior of Beams without Shear Reinforcement

High shear stress causes formation of inclined cracks in a beam. This is especially true for beams having only longitudinal reinforcement. This type of reinforcement is designed to carry the tensile and compressive normal forces arising from bending moment. Shear reinforcement have to be used in order to prevent widening of inclined cracks.

An inclined crack occurring in a beam that was previously uncracked due to flexure is known as a web-shear crack. An inclined crack originating at the top of and becoming an extension to a previously existing flexural crack is known as a flexure-shear crack. The critical flexural crack is referred to as the initiating crack (Wang and Salmon, 1979).

Web-shear cracks are relatively rare, particularly seen in non-prestressed beams and also these cracks occur in thin-webbed I-shaped beams. Flexural cracks are common both in reinforced and prestressed concrete. The flexural cracks, usually expanding approximately vertically into the beam, cause no distress to the beam until a critical combination of flexural and shear stresses develop near the interior extremity of one of the cracks. After that, inclined crack forms. The rate of transformation of the initiating flexural crack into the flexure-shear crack depends on the rate of growth and height of flexural cracks, as well as the magnitude of shear stresses acting near the tops of flexural cracks(Wang and Salmon, 1979).

The transfer of shear in reinforced concrete members occurs by a combination of the following mechanisms, as shown in Figure 2.3.

Following parameters (as shown in Figure 2.3) contribute to shear resistance of reinforced concrete beams:

- Shear resistance of the uncracked concrete, V_{cz}
- Aggregate interlock or interface shear transfer force V_a, tangentially along a crack,

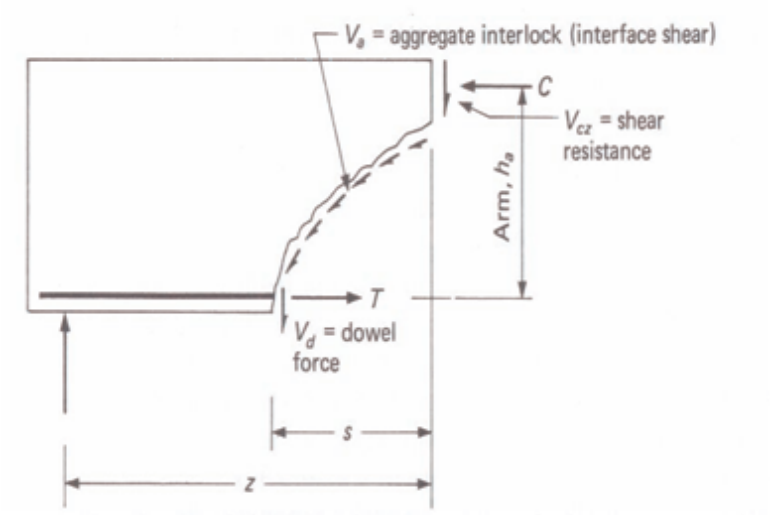

Figure 2.3. Redistribution of shear resistance after formation of inclined crack (Wang and Salmon, 1979).

and similar to a frictional force due to irregular interlocking of the aggregates along the rough concrete surfaces on each side of the crack.

- Dowel action, V_d, the resistance of the longitudinal reinforcement to a transverse force.
- Arch action on relatively deep beams.
- Shear reinforcement resistance, V_s, from vertical or inclined stirrups (not available in beams without shear reinforcement) (Wang and Salmon, 1979).

2.3. Types of Failure Mode with Different Shear Span-to-Effective Depth Ratio

Four general categories of failure may be established:

i Deep beams with $a/d < 1$.

ii Short beams with a/d ratios from 1 to about 2.5, in which the shear strength exceeds the inclined cracking capacity.

iii Usual beams of intermediate length having a/d ratios from about 2.5 to 6, in which the shear strength equals the inclined cracking strength.

iv Long beams with a/d greater than 6, whose flexural capacity is less than their

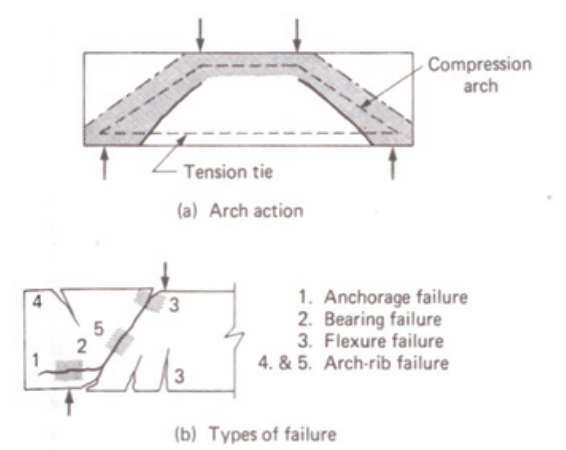

Figure 2.4. Modes of failure in deep beams, a/d $\leq$ 1 (Wang and Salmon, 1979).

concrete shear strength.

In deep beams ($a/d \leq 1$) shear stress has the predominant effect. After inclined cracking occurs, this beam tends to behave like a tied-arch wherein the load is carried by direct compression extending around the shaded area of Figure 2.4, ($a/d \leq 1$) and by the tension in the longitudinal steel. Once the inclined crack develops, the beam transforms quickly into a tied-arch which exhibits considerable reserve capacity. Several modes of failure are possible for the tied-arch system, as shown in Figure 2.4 (Wang and Salmon, 1979).

In Figure 2.4, numbers show following failure modes; (1) an anchorage failure; that is, pullout of the tension reinforcement at the support; (2) a crushing failure at the reactions; (3) a flexure failure arising from either a crushing of concrete near the top of the arch or a yielding of the tension reinforcement; (4) failure of the arch rib due to an eccentricity of the arch thrust, resulting in either a tension crack over the support at point 4 of Figure 2.4 or a crushing of concrete on the underside of the rib at point 5 (Wang and Salmon, 1979).

Similar to deep beams, for short beams ($1 < a/d < 2.5$) the ultimate shear capacity also exceeds the inclined cracking capacity. Failure occurs at some load higher than that which caused the inclined crack. After the flexure-shear crack develops, the crack extends further into the compression zone as the load increases. It also

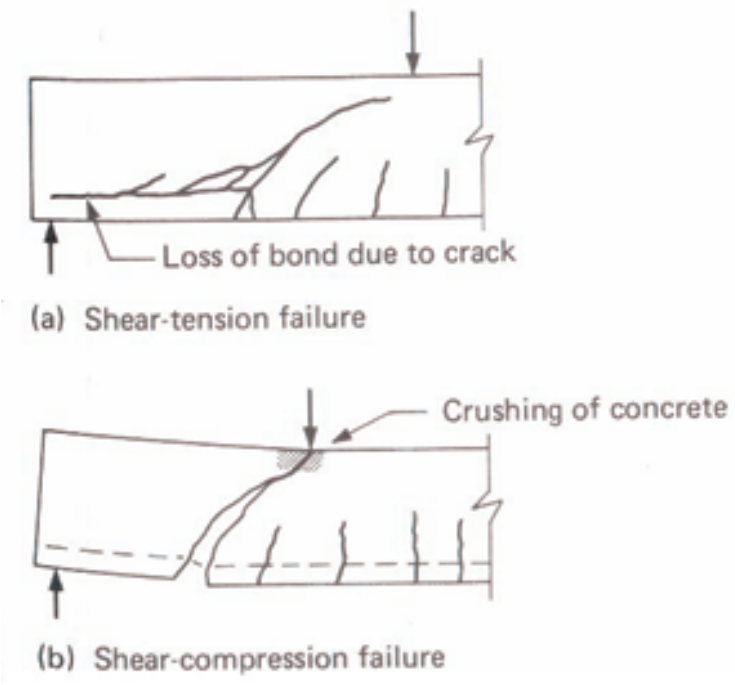

Figure 2.5. Typical shear failures in short beams, a/d = 1 to 2.5 (Wang and Salmon, 1979).

propagates as a secondary crack toward the tension reinforcement and then progresses horizontally along that reinforcement. Failure results from an anchorage failure at the tension reinforcement, called a shear tension failure (Figure 2.5) or a crushing failure in the concrete near the compression face, called a shear compression failure (Figure 2.5) (Wang and Salmon, 1979).

For intermediate length beams ($2.5 < a/d < 6$), first vertical cracks form, followed by the inclined flexure-shear cracks. At the beginning, several flexural cracks tend to bend over creating beam segments between cracks like "teeth" shown in Figure 2.6 (Wang and Salmon, 1979) . As a result of the increasing number of flexural cracks, when the root of the "tooth" is so reduced in size that it becomes unable to carry the moment arising from $\triangle T$, it breaks to form the inclined flexure-shear crack. At the sudden occurrence of the inclined crack, the beam is not able to redistribute the load, as in the situation of smaller a/d ratio. In other words, the formation of the inclined crack represents the ultimate shear capacity of beams in this category, for which the term "diagonal tension failure" has been given (Wang and Salmon, 1979).

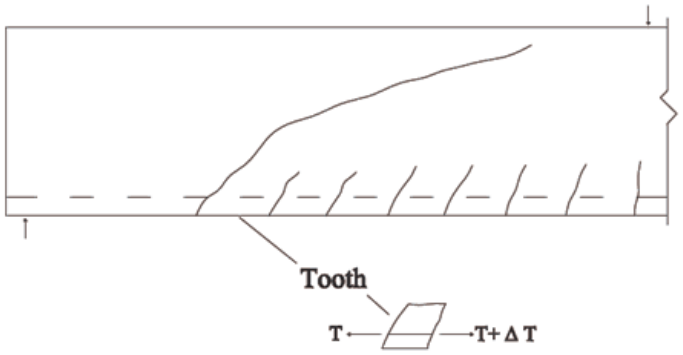

Figure 2.6. Diagonal Tension Failure on intermediate length beams (Wang and Salmon, 1979).

At $a/d > 6$, the failure of long beams starts with yielding of the tension reinforcement and ends by crushing of the concrete at the section of maximum bending moment. In addition to the nearly vertical flexural cracks at the section of maximum bending moment, slightly inclined (from the vertical) cracks may be present before failure between the support and the section of maximum bending moment. However, the ultimate strength of the beam is wholly dependent on the magnitude of the maximum bending moment and is not influenced by the size of the shear force (Wang and Salmon, 1979).

2.4. Fibre Reinforced Concrete (FRC)

Fibre reinforced concrete (FRC) may be defined as a composite material made with Portland cement, aggregate, incorporating discontinuous fibres which increases reinforced concrete's structural integrity. It contains short discrete fibres that are uniformly distributed and randomly oriented. Fibers could be made using different materials such as steel, glass, polypropylene, etc. Properties of composite material depend on fiber type, fiber geometry, fiber volume, and fiber dispersion state (Shah and Batson, 1987).

One of the most used types of fibers is steel fibers. Various parameters are used to describe the steel fibers. These are fiber aspect ratio (l_f/d_f), fiber tension-fraction strength and geometry.

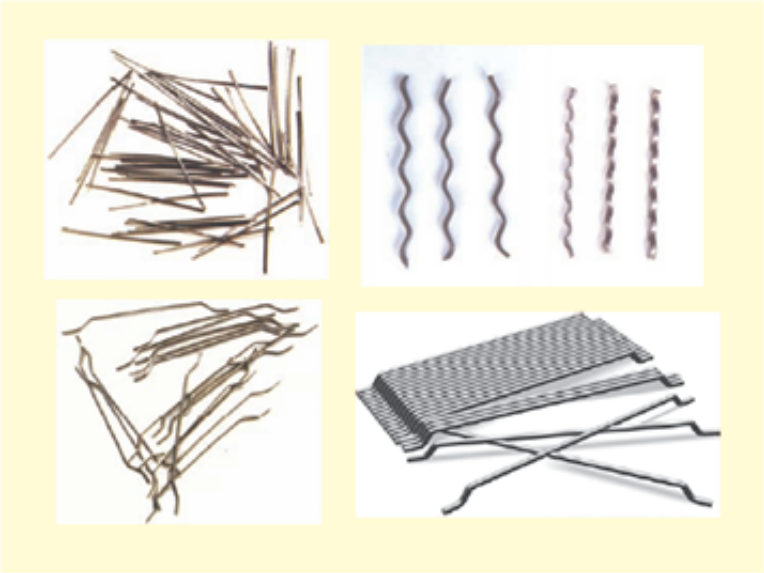

Figure 2.7. Various types of steel fibres (Yerlikaya, 2005).

There are several types of steel fibres that are used in construction. Some of them are seen in Figure 2.7. They may have different shape and geometry such as straight fibers, hooked end fibers, crimped fibers or deformed fibers.

For steel fibres, usually three different variables are used to control the fibre performance: (1) aspect ratio, (2) fibre shape, geometry and surface deformation (to count in the effect of anchorage), and (3) fiber tensile strength. Commonly used steel fibres have round cross-section, diameters varying from 0.2 to 1 mm, length ranging from 10 to 60 mm, and an aspect ratio less than 100 (typically ranging from 40 to 80). Fibres often have some specific geometry (such as hooked ends) to increase their performance. (Lofgren, 2005).

2.4.1. Steel Fibre Reinforced Concrete (SFRC)

2.4.1.1. General. Steel fibre reinforced concrete is a composite material having fibres as the additional ingredient. Small percentages of fibers are randomly dispersed in plain concrete. SFRC products are manufactured by adding steel fibres to the ingredients of concrete in the mixer and by transferring the fresh concrete into moulds. The product is then compacted and cured by the conventional methods. Segregation or balling is one of the problems encountered during mixing and compacting SFRC. This should be

avoided for random distribution of fibres. The energy required for mixing, conveying, placing and finishing of SFRC is slightly higher (Mishra, 2009).

Steel fibres are added to concrete to improve the structural properties, particularly tensile and flexural strength. The extent of improvement in the mechanical properties achieved with SFRC over those of plain concrete depends on several factors, such as shape, size, volume, percentage and distribution of fibres
(Mishra, 2009).

2.4.1.2. History of SFRC. Steel fibre reinforced concrete (SFRC) was introduced commercially into the European market in the second half of the 1970's. No standards or recommendations were available at that time which was a major obstacle for the acceptance of this new technology. Initially steel fibres were mostly used as a substitute for secondary reinforcement or for crack control in less critical parts of the construction. Today steel fibres are widely used as the main and unique reinforcement for industrial floor slabs, shotcrete and prefabricated concrete products. They are also considered for structural purposes in reinforcement of slabs on piles, full replacement of the standard reinforcing cage for tunnel segments, concrete cellars, foundation slabs and shear reinforcement in prestressed elements. (Steel fibre reinforced concrete (SFRC) - Quality, performance and specification BOSFA).

2.4.1.3. Technology for Producing SFRC. SFRC can, in general, be produced using conventional concrete practice, though there are obviously some important differences. The basic problem is to introduce a sufficient volume of uniformly dispersed fibers to achieve the desired improvements in mechanical behavior, while retaining sufficient workability in the fresh mix to permit proper mixing, placing and finishing. The performance of the hardened concrete is enhanced more by fibres with a higher aspect ratio, since this improves the fibre-matrix bond. On the other hand, a high aspect ratio adversely affects the workability of the fresh mix. In general, the problems of both workability and uniform distribution increase with increasing fibre length and volume (Chanh, 2005).

One of the chief difficulties in obtaining a random fibre distribution is the tendency of steel fibres to ball or clump together. Clumping may be caused by a number of factors:

i The fibres may already be clumped together before they are added to the mix; normal mixing action will not break down these clumps.
ii Fibres may be added too quickly to allow them to disperse in the mixer.
iii Too high a volume of fibres may be added.
iv The mixer itself may be too worn or inefficient to disperse the fibres.
v Introducing the fibres to the mixer before the other concrete ingredients will cause them to clump together (Chanh, 2005).

In view of this, care must be taken in the mixing procedures. Most commonly, when using a transit mix truck or revolving drum mixer, the fibres should be added last to the wet concrete. The concrete alone, typically, should have a slump of 50-75 mm greater than the desired slump of the SFRC. Of course, the fibres should be added free of clumps, usually by first passing them through an appropriate screen. Once the fibres are all in the mixer, about 30-40 revolutions at mixing speed should properly disperse the fibres. Alternatively, the fibres may be added to the fine aggregate on a conveyor belt during the addition of aggregate to the concrete mix. The use of collated fibres held together by a water-soluble sizing which dissolves during mixing largely eliminates the problem of clumping (Chanh, 2005).

SFRC can be placed adequately using normal concrete equipment. It appears to be very stiff because the fibres tend to inhibit flow; however when vibrated, the material will flow readily into the forms. It should be noted that water should be added to SFRC mixes to improve the workability only with great care, since above a w/c ratio of about 0.5, additional water may increase the slump of SFRC without increasing its workability and place ability under vibration. The finishing operations with SFRC are essentially the same as for ordinary concrete, though perhaps more care must be taken regarding workmanship (Chanh, 2005).

2.4.1.4. Structural Use of SFRC . As recommended by ACI Committee 544, 'when used in structural applications, steel fibre reinforced concrete should only be used in a supplementary role to inhibit cracking, to improve resistance to impact or dynamic loading, and to resist material disintegration. In structural members where flexural or tensile loads will occur, the reinforcing steel must be capable of supporting the total tensile load'. Thus, while there are a number of techniques for predicting the strength of beams reinforced only with steel fibres, there are no predictive equations for large SFRC beams, since these would be expected to contain conventional reinforcing bars as well. An extensive guide to design considerations for SFRC has recently been published by the American Concrete Institute. In this section, the use of SFRC will be discussed primarily in structural members which also contain conventional reinforcement.

For beams containing both fibres and continuous reinforcing bars, the situation is complex, since the fibres act in two ways:

i They permit the tensile strength of the SFRC to be used in design, because the matrix will no longer lose its load-carrying capacity at first crack; and
ii They improve the bond between the matrix and the reinforcing bars by inhibiting the growth of cracks emanating from the deformations (lugs) on the bars.

However, it is the improved tensile strength of SFRC that is mostly considered in the beam analysis, since the improvements in bond strength are much more difficult to quantify. Steel fibres have been shown to increase the ultimate moment and ultimate deflection of conventionally reinforced beams; the higher the tensile stress due to the fibres, the higher the ultimate moment (Chanh, 2005).

2.4.1.5. Previous Studies on Shear Strength of Fiber Reinforced Concrete. Narayanan R. and Darwish I. Y. S. made investigations (Narayanan and Darwish, 1987) on the behavior of steel fiber reinforced concrete beams subjected to predominant shear in 1987. The results of some 49 shear tests carried out on simply supported rectangular beams under symmetrically placed concentrated loads are presented and analyzed; of

these, 10 beams contained conventional stirrups and 33 were reinforced with crimped steel fibers as web reinforcement. The parameters were the volume fraction V_f of the fibers, fiber aspect ratio l/d, concrete strength f_c, amount of longitudinal reinforcement ρ, and the shear span/effective depth ratio a/d. The test results show that the first crack shear strength increased significantly due to the crack-arresting mechanism of the fibers; the improvements in ultimate shear strength were of the same order as that obtained from conventional stirrups even for a fiber volume fraction of 1%. Any further increase in fiber contents did not result in corresponding improvements in the shear strengths.

Furlan Jr. et al. conducted a study (Junior and Hanai, 1997) in 1996. This study was related with shear/flexure tests on steel and polypropylene fiber reinforced concrete beams. In addition to analyzing the influence of fibers on the structural performance in situations of different ratios of shear reinforcement, some aspects of the properties of fresh and hardened concrete are introduced. Fourteen square-section beams (100∗100∗1000 mm) were tested. The beams were prepared from seven different mix proportions, varying the type and the volume of fiber added. There were two beams for each mix: one model with stirrups and the other without stirrups. The main alterations resulting from the use of fibers were increased shear strength, stiffness and ductility. Other parameters used in analyzing performance were the properties of the hardened concrete (compressive strength, tensile strength, and modulus of elasticity), and stresses in the stirrups, in the longitudinal reinforcement and in the concrete (at the web and compression zone).

In 1997, Kützing conducted a test program at the University of Leipzig. This test program is carried out to find out the effects of steel fibres on the ductility and the ultimate shear strength of concrete. He tested 3 series of beams: the NSC and the HSC beams without fibres and one NSC beam with 40 kg/m$_3$ of steel fibres. The longitudinal reinforcement ratio was 1.57%. He tested 3 series of beams: the NSC and the HSC beams without fibres and one NSC beam with 40 kg/m$_3$ of steel fibres. The beams were loaded in 4 points with a total span of 1.54 m. Test results indicated that when 40 kg/m$_3$ were added to the NSC, the shear capacity rose very strongly according

to the plain NSC and HSC beams. The shear strength surpassed the ultimate bending capacity of the test beam (Kutzing, 1997).

A study was made by Lim et al. (Lim, 1999) in 1997. In this study, a total of nine beams have been tested to investigate the influence of fibre reinforcement on the mechanical behavior of reinforced concrete beams in shear. The major test variables are the volume fraction of steel fibres and the ratios of stirrups to the required shear reinforcement. The fibre volumes were varied from 0% to 2% and the amount of stirrups varied from zero to the amount of the required shear reinforcement. The test results show that the first crack shear strength increases significantly as fibre content increases and the improvement in ultimate shear strength is also achieved. At the end, the authors showed that fibre reinforcement can reduce the amount of shear stirrups required and that the combination of fibres and stirrups may meet strength and ductility requirements. They also showed that the mode of failure changed from shear to flexure when the volume fraction of steel fibres used exceeds a certain amount, about 1%. This means that addition o fibre reinforcement increases shear capacity greatly.

J. K. Oh and S. W. Shin made an experiment (Oh and Shin, 2001) about shear strength of reinforced High-Strength Concrete Deep Beams. In their study, fifty-three reinforced concrete deep beams with compressive strengths in the range from 23 to 74 MPa were tested to determine their diagonal cracking and ultimate shear capacities symmetrically under two-point loading. The shear span-effective depth ratio a/d varied from 0.5 to 2.0. The reinforcement ratio was varied from one group to another one. The ultimate shear failure mode of deep beams was governed by a/d regardless of concrete strength. At lower a/d, deep beams with high-strength concrete failed abruptly without any caution, which could be seen in deep beams with normal-strength concrete. But no significant change in the failure mode was observed between normal and high-strength concrete deep beams. Also test results indicate that the ultimate shear strength of deep beams was determined predominantly by a/d.

Majdzadeh, Soleimani and Banthia (Majdzadeh, Soleimani and Banthia, 2006)

investigated the influence of fiber reinforcement on the shear capacity of reinforced concrete (RC) beams in 2006. They investigated steel and synthetic fibers at variable volume fractions. They performed two series of tests. One is structural tests, where RC beams were tested to failure under an applied four-point load. Other is materials tests, where companion fiber-reinforced concrete (FRC) prisms were tested under direct shear to obtain material properties such as shear strength and shear toughness. Fiber-reinforced concrete test results indicated an almost linear increase in the shear strength of concrete with an increase in the fiber volume fraction. Fiber reinforcement enhanced the shear load capacity and shear deformation capacity of RC beams, but 1% fiber volume fraction was seen as optimal; no benefits were noted when the fiber volume fraction was increased beyond 1% .

In 2007, test data were presented on the shear strength of a series of reinforced cement concrete (RCC) deep beams by Madan, Kumar and Singh, 17. Beams properties had three steel fiber volume fractions ($0, 1.0$ and 1.25%, three shear span to effective depth ratios (0.75, 1.0 and 1.25) and three combinations of web reinforcement. A total of 18 simply supported deep beams were tested to failure under two-point top loading. All beams were of rectangular cross section, 90 mm wide and 260 mm deep with 2 bars of $10mm$ diameter as longitudinal reinforcement. The effective span to overall depth ratio was changed from 1.69 to 2.5, in order to achieve the desired shear span-to-effective depth ratio (a/d). The steel fibers used in the investigation were of diameter of 0.45 mm and length of 40.5 mm, straight in length having an aspect ratio of 90. In this study, the test results indicated that the fibers have important effect on the shear strength of a longitudinally reinforced concrete beams. Shear strength increased with increasing fiber volume and decreasing shear span to-effective depth ratio. The authors stated that the steel fibers can replace the conventional web reinforcement in RCC deep beams.

In 2008, Salna and Marciukaitis made an experimental research (Arslan, 2008) about the influence of steel fibre volume and shear span ratio on the strength of fibre reinforced concrete elements in various states of stress. Thirty six beams with three different shear spans (a/h $= 1, 1.5$, and 2% and three different fibre volumes (1, 1.5, and

2% were tested to examine how these factors influence the behavior of such elements. The cross-section of beams were b x h =100 × 200 mm, and length l = 500; 750; 1000mm. Test results show that plasticity, crack propagations and load capacity of elements are greatly influenced by steel fibre volume and shear span. Load capacity of tested beams, in variation of volume fraction at different a/h, is different. When a / h = 1, load capacity grows from 1.62 to 1.89 times. At higher values of shear span ratio, the increase of load capacity is not so significant. For example, when a / h = 1.5 and a / h = 2, the increase from 1.26 to 1.56 and 1.14 to 1.54 times.

In 2008, Greenough and Nehdi performed an investigation (Greenough and Nehdi, 2008) on the shear behavior of fiber-reinforced self-consolidating concrete beams. These beams were designed to see the influence of fiber type, fiber anchorage, fiber aspect ratio, and fiber content on the shear performance of reinforced concrete slender beams without stirrups, and to determine the suitability of using fibers to satisfy minimum shear reinforcement requirements. The specimens include different types and sizes of fibers. Varying percentages (0.5, 0.75, or 1.0) of hooked end, flat end, or wavy fibers with different lengths (30 and 50 mm) were used. The beam specimens were 200 x 300 x 2400 mm in size with a reinforcement depth and ratio of 265 mm and 1.7%, respectively. Test results showed that SCC is particularly well suited for fiber addition owing to its inherent fresh properties. In this study, the maximum fiber addition was 1% because producing FR-SCC with fiber volumes above 1% is difficult. Moreover, the maximum shear capacity of reinforced SCC slender beams without stirrups can be significantly enhanced with fiber addition. For 1% steel fiber volumes, increases in shear capacity by up to 128% over that of the reference mixture were achieved. The energy absorption of reinforced SCC slender beams without stirrups was significantly improved by the addition of steel fibers, reaching as much as six times that of the reference beam with no fibers for beams with a 1% fiber volume. FR-SCC beams without stirrups displayed superior shear performance compared with that of conventional FRC beams without stirrups, because better workability and the elimination of mechanical vibration led to a more homogeneous dispersion of fibers.

Another study was conducted by Mansur et al. (Mansur, 1986) in order to investi-

gate shear behavior of reinforced fibrous concrete. In this study, test data are presented on the shear strength of a series of longitudinally reinforced fibrous concrete beams in which the shear span-to-effective depth ratio, volume fraction of fibers, percentage of reinforcement, and strength of the concrete were varied. Test results indicated that the fibers have significant influence on the mode of failure and ultimate shear strength of a longitudinally reinforced concrete beam. Moreover, shear strength increases with increasing fiber content and decreasing a/d ratio. For a particular volume fraction of fibers, the rate of increase in shear strength is higher at low values of a/d.

Yang K. H. (Yang, 2003) conducted an experimental study to interpret the shear characteristics of high-strength concrete deep beams including size effects of beam section and evaluate the validity of the ACI code. Twenty-one beam specimens were tested to investigate their shear characteristics with the variables of concrete strength, shear span/depth ratio, and overall depth. The decrease in shear span/depth ratio and the increase in overall depth under the same shear span/depth ratio led to more brittle failure, with wide diagonal cracks and high energy release rate related to size effects. The high-strength concrete deep beams exhibited more remarkable size effects with regard to brittle behavior.

3. EXPERIMENTAL PROGRAM

3.1. Specimen Details

Ten slender beam specimens with two shear span-to-effective depth ratio (a/d = 2.00 and 3.75) were tested for this study in order to investigate the influence of the strength of concrete, shear span-to-depth ratio, fibre type and fibre volume fraction on the shear resistance of beams without web reinforcement.

Previous study (Wang and Salmon, 1979) shows that different failure modes are obtained for the varying values of a/d as given below: If;

- $a/d < 1.5$: beams behave like a tied arch,
- $a/d > 7$: behavior is expected to be dominated by flexure
- $1.5 < a/d < 2.5$: shear-compression failure is observed
- $2.5 < a/d < 6$: diagonal tension failure is observed.

Since the objective of this study is to examine shear behavior of fiber reinforced concrete beams, two shear span-to-depth ratios (2 and 3.75) which are expected to yield shear related failure were chosen.

Hybrid fiber combination was used in high strength concrete. Two different fibers were used. Both fibers have hooked-ends and have lengths and aspect ratios of 35/65 and 60/80 mm, respectively. Five different fibre-volume fractions were chosen; $V_f = 0, 0.5, 0.75, 1.00$ and 1.50%. The hybrid combinations are given in table 3.1.

Table 3.1 also shows the details of the test beams. All of the beams had the same cross-sectional area (125 x 250 mm) with an effective depth of 212 mm and the same longitudinal reinforcement ($2\phi16$ bars). The dimensions and longitudinal reinforcement content of the beams correspond to an approximate longitudinal reinforcement ratio of 1.5%. In addition, total length of the beams is 2300 mm. Two top-bars with a length

of 20 cm were used at each support. The top-bars were enclosed to the flexural bars by four 10 stirrups at each end to prevent the possibility of anchorage failure. There were no stirrups in the shear span as shown in Figure 3.1.

Table 3.1. Summary of Experimental Program.

Specimen	Concrete Type	Longitudinal Reinforcement Ratio (ρ)	Volume Fraction ($V_f, \%$)	Fibre Type	Aspect Ratio of Fibre(l/d)	f_{ck} (Mpa)	a/d
B-01	HSC	$2\phi16 - 1.5\%$	0.00	-	-	59.27	2.00
B-02	HSC	$2\phi16 - 1.5\%$	0.00	-	-	59.27	3.75
B-03	HSC	$2\phi16 - 1.5\%$	0.25 + 0.25	RC-65/35-BN RC-80/60-BN	$35/0.55 = 65$ $60/0.75 = 80$	39.11	2.00
B-04	HSC	$2\phi16 - 1.5\%$	0.25 + 0.25	RC-65/35-BN RC-80/60-BN	$35/0.55 = 65$ $60/0.75 = 80$	39.11	3.75
B-05	HSC	$2\phi16 - 1.5\%$	0.25 + 0.50	RC-65/35-BN RC-80/60-BN	$35/0.55 = 65$ $60/0.75 = 80$	39.51	2.00
B-06	HSC	$2\phi16 - 1.5\%$	0.25 + 0.50	RC-65/35-BN RC-80/60-BN	$35/0.55 = 65$ $60/0.75 = 80$	39.51	3.75
B-07	HSC	$2\phi16 - 1.5\%$	0.50 + 0.50	RC-65/35-BN RC-80/60-BN	$35/0.55 = 65$ $60/0.75 = 80$	39.58	2.00
B-08	HSC	$2\phi16 - 1.5\%$	0.50 + 0.50	RC-65/35-BN RC-80/60-BN	$35/0.55 = 65$ $60/0.75 = 80$	39.58	3.75
B-09	HSC	$2\phi16 - 1.5\%$	0.75 + 0.75	RC-65/35-BN RC-80/60-BN	$35/0.55 = 65$ $60/0.75 = 80$	38.71	2.00
B-10	HSC	$2\phi16 - 1.5\%$	0.75 + 0.75	RC-65/35-BN RC-80/60-BN	$35/0.55 = 65$ $60/0.75 = 80$	38.71	3.75

Figure 3.1. Image of beam reinforcement.

3.2. Materials

3.2.1. Concrete Mixture Design

Concrete mix was prepared in Akçansa Mahmutbey ready-mixed concrete plant in Küçükçekmece and casting was done in Boğaziçi University Civil Engineering Laboratory. Only one type of concrete mixture was prepared and fibers fed into the concrete mixture to obtain fiber-reinforced concrete mixtures with different fiber volume fractions. High Strength Concrete (HSC) was used. Small value of w/c ratio is needed to produce high strength concrete. The mixture design values for the HSC are shown in Table 3.2. Casting of concrete is shown in Figure 3.2.

In order to determine the compressive strength of concrete in accordance with TS500 (TS-500, Betonarme Yapıların Hesap ve Yapım Kuralları, Turkish Standards, 2007), cylinder samples with a diameter of 150 mm and heights of 300 mm were used. Before compression tests, shaving has to be done on the surface of HSC cylinder specimen, since sulfur capping is not suggested due to the controversy of strength between specimen and sulfur. Sulfur capping crushes before concrete and it does not distribute the load to whole area properly. The concrete on the shaving machine and compression test machine are shown in the following figures.

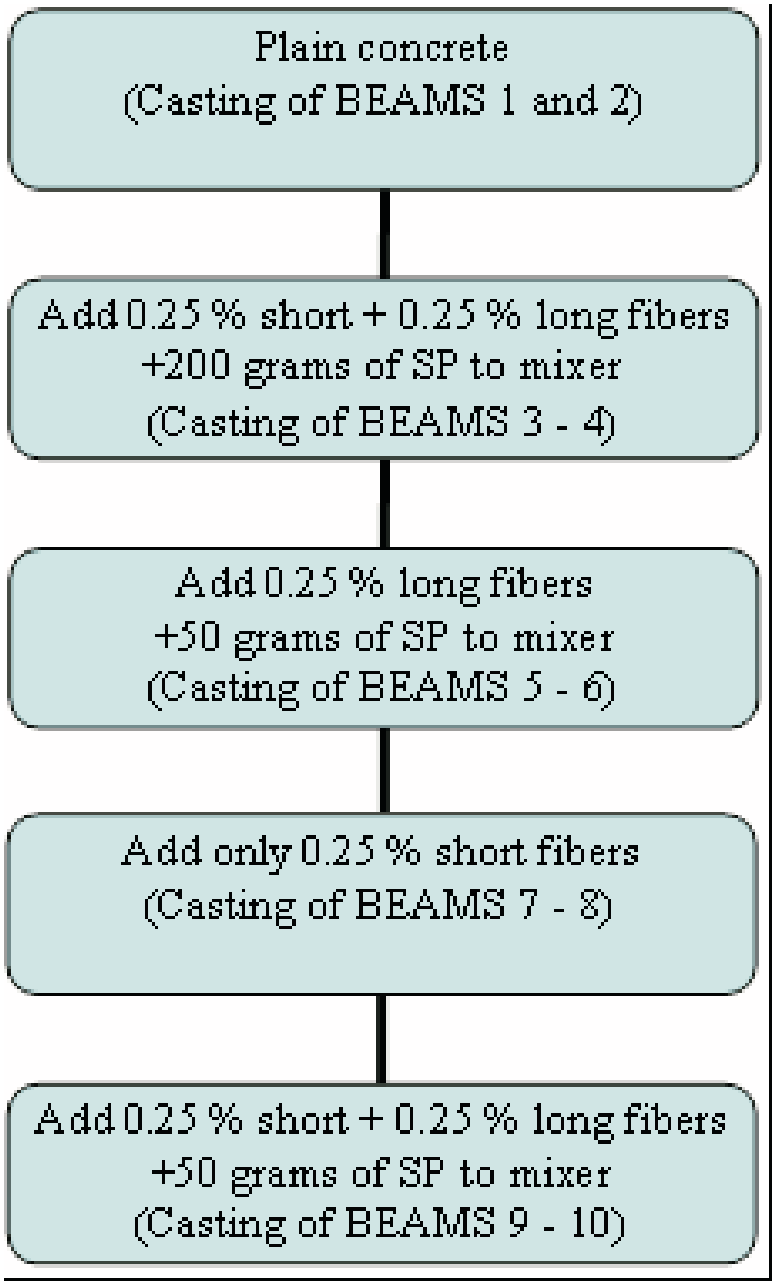

Figure 3.2. Casting of Concrete Scheme.

Table 3.2. High strength concrete mixture design.

Material	Weight for m^3 (kg/m^3)
Cement (CEM I 42.5R)	600
Water	180
Sand (0-4mm)	230
No 0 Aggregate (0-5 mm)	200
No 1 Aggregate (5-12 mm)	695
No 2 Aggregate (12-22 mm)	485
Super plasticizer	10.8
Unit Weight (kg)	2400.8
w/c	0.3

Figure 3.3. Compression Test Machine.

Table 3.3. Properties of RC-80/60-BN and RC-65/35-BN.

FIBRE TYPE	LENGTH (MM)	DIAMETER (MM)	ASPECT RATIO (L/D)	MIN. TENSILE STRENGTH (MPA)	FIBRES / KG
RC-80/60BN	60	0.75	80	1,050	4,600
RC-65/35-BN	35	0.55	65	1,100	14,500

3.2.2. Reinforcing Steel

$\phi 16$ ribbed bars with a characteristic yield strength of 420 MPa were used for the longitudinal reinforcement. Also ribbed bars with $\phi 10$ were used as stirrups.

3.2.3. Steel Fibres

Two types of fibres were used in the experiment. First one is $RC-65/35-BN$ which is a cold drawn wire fibre, with hooked ends. It has a length of 35 mm and diameter of 0.55 mm (aspect ratio is 65). Second one is RC-80/60-BN. First value indicates aspect ratio (l/d) and second value is length. It has a diameter of 0.75 mm. Fibres were added to trans-mixer step by step in order to reach different volume fraction for five groups of beam. The properties of the two types of fibres are given in Table 3.3, respectively.

3.2.4. Test Procedure

Four-point loading tests were carried out in Boğaziçi University Structures Laboratory. All the beams were supported by a hinge on one end and a roller at the other end as shown in Figure 3.4. Two equal loads were symmetrically applied to the beams using steel profiles and two 80 mm-wide loading plates. The loading capacity is 20 tons in frame. Loading is applied by manual hydraulic jack. After, hydraulic pump pressed the beams. The increment in load and mid-span deflection were recorded for

Figure 3.4. Test Setup.

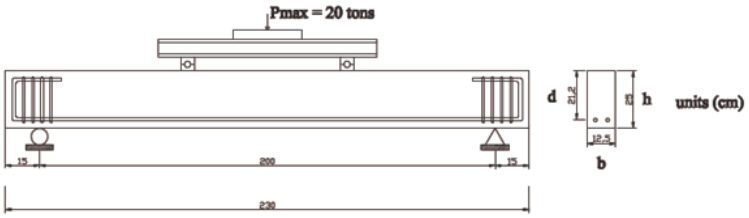

Figure 3.5. Sketch of the Test set-up.

each second. An LVDT (linear variable displacement transducer) was used to measure the midspan displacement. The beams were painted white before testing in order to observe cracks accurately. The first cracking load of each beam was noted and crack propagation was showed by red lines.

The sketch of test set-up is shown in Figure 3.5.

4. EXPERIMENTAL RESULTS

4.1. General

In this section, the results of tests are presented. Observations and mathematical results were presented to characterize the shear behavior of fibre-reinforced concrete beam specimens.

4.2. Test Results

4.2.1. Concrete tests on small size specimens

4.2.1.1. Compression Test. Compressive strength results obtained from cylindrical specimens are given in Table 4.1. As it is seen in Table 4.1 compressive strength of the specimens decreased with addition of fibers. This was unexpected since previous studies show that fiber effect on compressive strength is not pronounced. However, during this study, all the beams (with or without fibers) were cast from the same mixer and no internal vibration is applied not to disturb fiber dispersion state. Because, internal vibrators used to place concrete is known to cause unreinforced regions in structural elements. Therefore, placement of concrete is done by hammering the moulds from outside. Fiber addition was completed in 5 steps (see Figure 3.2 and Table 3.2). Every time a certain amount of superplasticizer (approximately $50 - 200$ gr) was added into the mixer and the mixer was rotated until the desired flow properties were obtained. Workability of concrete was evaluated by doing slump test. Spreading of concrete was measured after adding fibers and superplasticizer each time and spreading values were kept higher than 30 cm. With an increased addition of fibers concrete workability decreased as expected. This resulted in a decreased placement performance and lower values of compressive strength were obtained from the fiber-reinforced specimens as is seen in Table 4.1. Discussion and evaluation of results were done by taking this effect into consideration as well as considering this effect as an important variable. While comparing the performances of fiber reinforced beams, the

Table 4.1. Compression Test Results of cylinder specimens.

Specimen	Volume Fraction (V_f%)	f_{ck} (MPa)	Concrete spread/slump (cm)
B-01	0.00	59.27	-
B-02	0.00	59.27	
B-03	60.25 + 0.25	39.11	55
B-04	0.25 + 0.25	39.11	
B-05	0.25 + 0.50	39.51	40
B-06	0.25 + 0.50	39.51	
B-07	0.50 + 0.50	39.58	35
B-08	0.50 + 0.50	39.58	
B-09	0.75 + 0.75	38.71	18 (slump)
B-10	0.75 + 0.75	38.71	

effect of compressive strength was not important since all the fiber reinforced beams yielded similar compressive strength values. However, normalized shear stress values ($V_{max}/\sqrt{f_c b_w} d$) were also calculated to exclude the effect of compressive strength when comparing unreinforced beams (B $1, 2$) with reinforced beams.

4.2.1.2. Four Point Bending Test. This test was done in order to obtain information about mechanical performance of small beam specimens and to relate results with the results obtained from the large size beams. The small beam specimens were tested under four-point bending, according to the test set-up shown in Figure 4.1 by using an MTS Closed-Loop Displacement Controlled Dynamic Testing Machine with 100 kN capacity. Loading was applied in displacement control. Displacement of stroke was used for vertical displacement of specimens. Two LVDTs were placed horizontally for measuring crack opening. Crack opening could be measured only when cracks formed in maximum moment region. Loading was performed controlling the displacement of the machine actuator, which was applied at a rate of 0.1 mm/min.

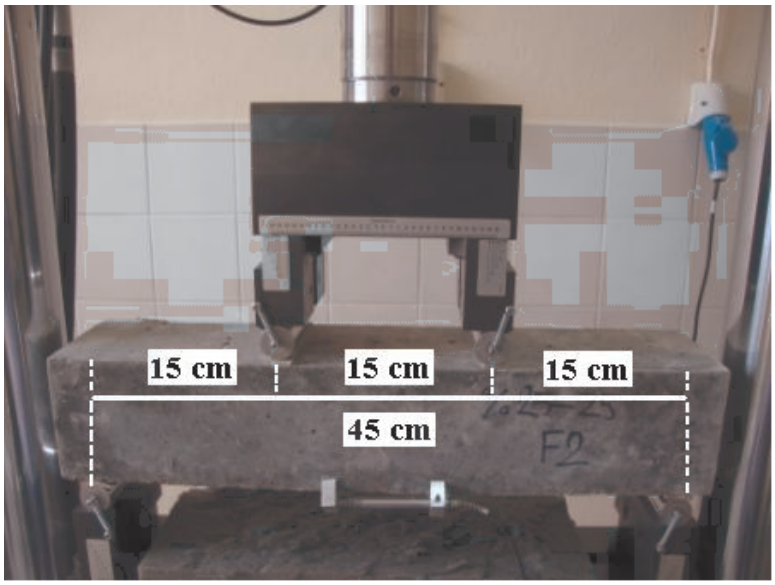

Figure 4.1. Four-point bending test setup.

Loading setup is given in Figure 4.1. Span length (L) was 450 mm and gap between the loading heads was 150 mm.

The results of four-point bending tests are given below in Figure 4.2. As can be seen from the figure, force vs. displacement behavior of specimens change with and increase in fiber content. For the plain specimens without fibers concrete shows brittle behavior and no post-peak response is recorded. On the other hand, when fibers are added to concrete, it shows ductile behavior either with a strain softening or strain hardening post-peak response. Transition from strain softening to strain hardening is seen when fiber volume increased to 0.75% and the specimens with higher fiber volume ratios ($1.00\% and 1.5\%$) show strain hardening behavior. It should be mentioned that the load bearing capacity was not found to change with an increase in fiber volume when 0.75% fiber volume was exceeded.

In Figure 4.2, the concavity of the nonlinear lines is not convenient with the true results. The concavity has to be downward because the stiffness of the concrete specimens decrease when the displacement increase. In this study stroke displacement of MTS was used and LVDT did not used vertically. However, the aim of this test is to compare mechanical behavior of small-size specimen with the behavior of large size beams. The relation with two types of beams is convenient according to the test

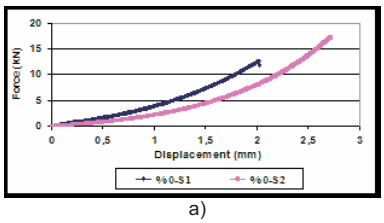

a)

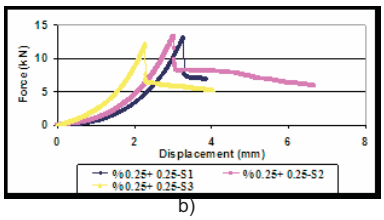

b)

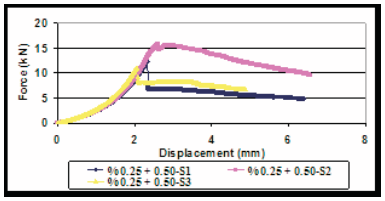

c)

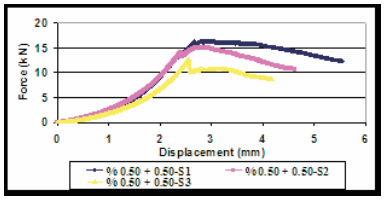

d)

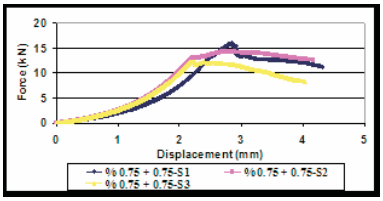

e)

Figure 4.2. Force vs. Displacement Curves for small size beam (100*100*500mm) specimens with various fiber contents (obtained from four-point bending) (fiber volume for a) 0%, b) 0.5%, c) 0.75%, d) 1.0% and e) 1.5%).

results.

Figure 4.3 shows force vs. average crack opening. These curves could be obtained only for some specimens. For other specimens a crack opened at regions out of the measuring range of LVDTs. Figure 4.3 also shows the positive effect of using fibers. Another result is that force vs. crack opening behavior of the specimens was not very much affected when fiber volume increased from 0.75 to 1.5%.

4.2.2. Tests on large scale specimens (Four-point Loading Test Results

4.2.2.1. $1B-01(V_f:0\%, a/d:2)$:. Shear compression type of failure is observed in this beam. It was failed by crushing of concrete above the diagonal crack, accompanied by a loud noise after the appearance of the inclined crack. The failure was brittle and sudden.

The first crack was a flexural crack in the mid-span region. When the loading was continued, cracks in the shear span began to get inclined. With further increase of load, the inclined crack progressed to the point of load application and to the supports of the beam. At this stage, a diagonal crack was fully developed. The beam continued to carry increased load with fully developed diagonal cracks. Finally, shear compression failure occurred by crushing of concrete below the load application point (Figure 4.4). The load-midspan deflection relationship for the B-01 is given in Figure 4.5.

The cracking and maximum shear stresses were found to be $1.08(V_{cr}/b_{wd})$ and $2.62(V_u/b_{wd})$ MPa. The maximum displacement was found as 8.90 mm.

4.2.2.2. $B-02(V_f:0\%, a/d:3.75)$:. Flexural cracks first appeared in the maximum moment region for this specimen. As the load was increased, second crack occurred in the shear span. With an increase in load, diagonal crack occurred in the shear span and progressed towards the load application point. With further increase in load, the inclined cracks began to progress downward to the level of longitudinal steel. Finally,

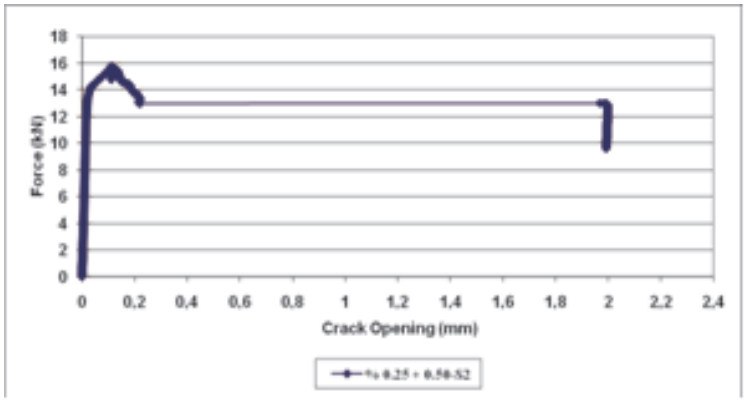

a)

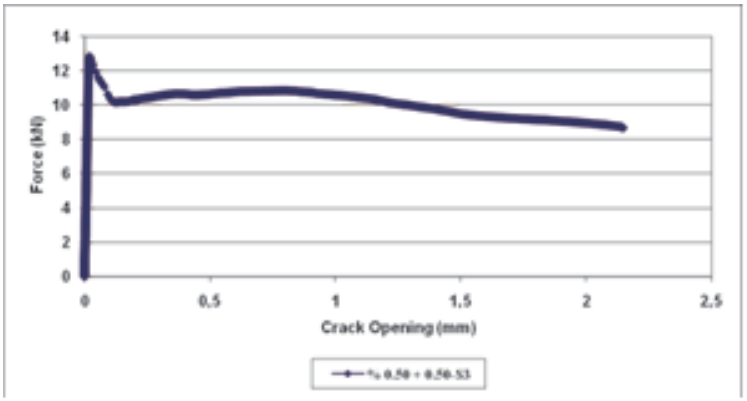

b)

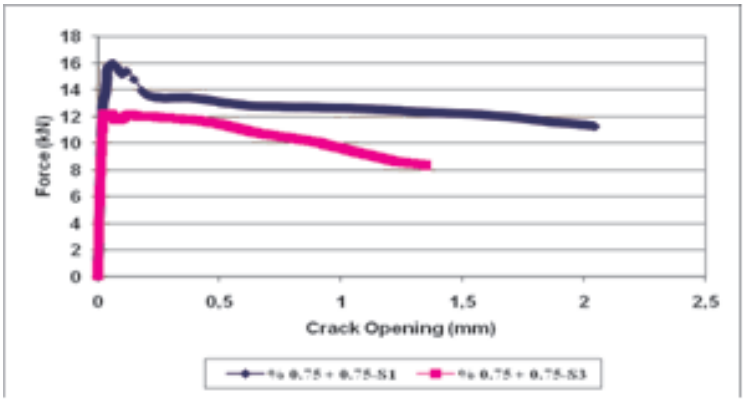

c)

Figure 4.3. Force vs. Average LVDT Displacement Curves for small size beam (100^*100^*500mm) specimens with various fiber contents (obtained from four-point bending). S1, S2 and S3 stand for different specimens (fiber volume a) 0.75%, b) 1.0% and c) 1.5%).

Figure 4.4. Damaged shape of B-01.

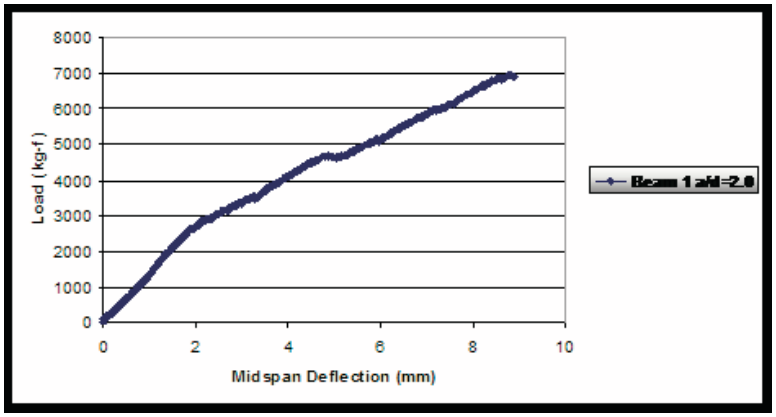

Figure 4.5. Load-Midspan deflection relationship for B-01.

Figure 4.6. Damaged shape of B-02.

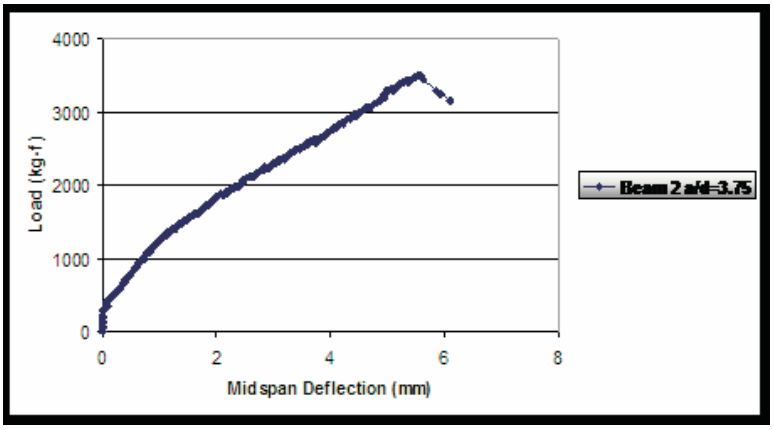

Figure 4.7. Load-Midspan deflection relationship for B-02.

the beam failed suddenly along the diagonal crack (Figure 4.6). The maximum stress was found as 1.32 MPa. The cracking stress was observed as 0.52 MPa. The maximum deflection before the beam failed by diagonal tension was found to be 6.1 mm (Figure 4.7).

4.2.2.3. $B-03(V_f : 0.25\% + 0.25\%, a/d : 2)$:. Similar to the B-01, B-03 showed a shear compression type of failure (Figure 4.8). It should be remembered that both Beams 01 and 03 had a shear span to depth ratio of 2.00. However, the number of cracks developed were different than B-01 (Figure 4.9). Due to the existence of fibres, lots of inclined cracks occurred in B-03. The cracking stress, maximum shear

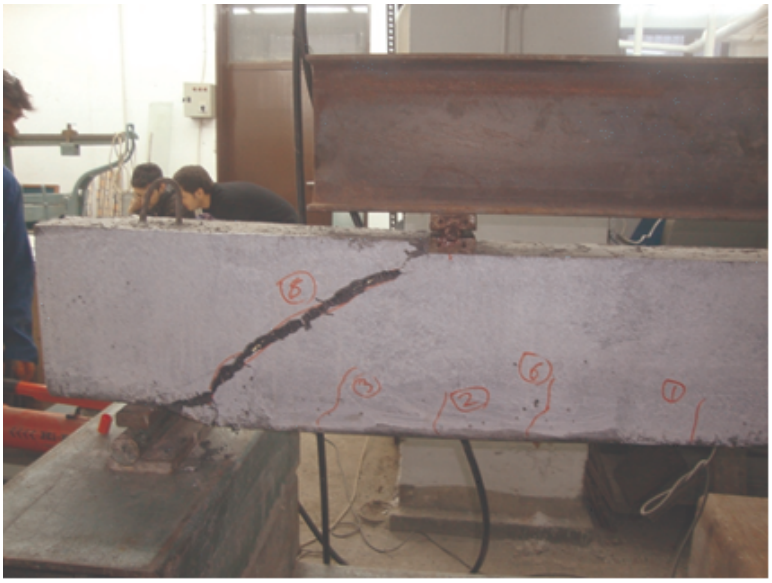

Figure 4.8. Damaged shape of B-03.

stress and maximum deflection values were found to be 1.08, 2.60 MPa, and 8.25 mm, respectively. Figure 4.10 shows load vs. mid-span deflection relation for B-03.

4.2.2.4. $B-04(V_f : 0.25\% + 0.25\%, a/d : 3.75)$:. In this beam, first, flexural cracks formed, then those cracks propagated vertically and accompanied by new cracks in the shear span. As the load was increased, some of the flexural cracks in the shear span were inclined towards the load application point similar to the B-02. Finally, diagonal tension failure occurred (Figures 4.11 and 4.12). The cracking stress was 0.42 MPa. The maximum stress carried by the beam was 1.49 MPa. It was observed that 0.5% fibre content increased the shear carrying capacity of the beam according to B-02. The maximum displacement was recorded as 7.43mm. Midspan deflection of this beam was higher than B-02. The load-midspan deflection relationship for the B-04 is given in Figure 4.13.

4.2.2.5. $B-05(V_f : 0.25\% + 0.50\%, a/d : 2)$:. As the other beams with a/d of 2.00 (B-01 and B-03), B-05 failed by shear compression (Figure 4.14 and 4.15). The maximum shear stress was larger than Beam 01 and 03. It was found as 3.60 MPa. The increase in fibre volume fraction from 0.5% to 0.75% increased the shear carrying capacity of the beam, significantly. The cracking stress and maximum displacement were

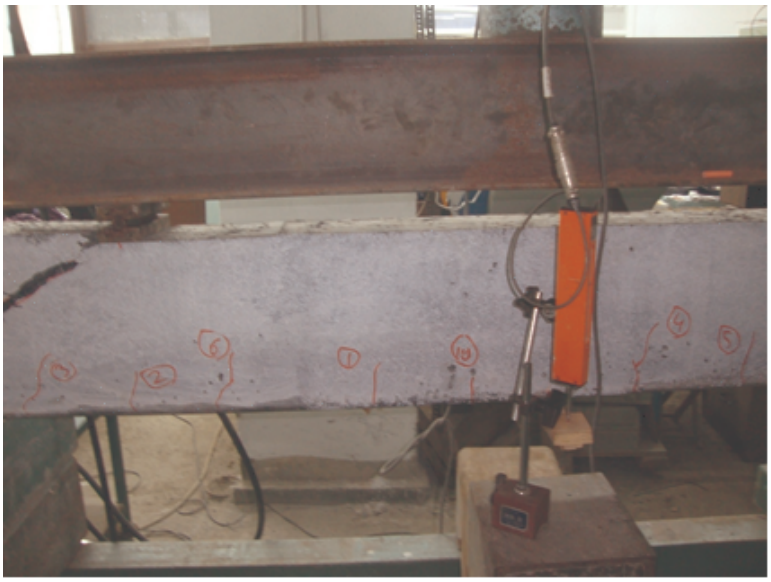

Figure 4.9. Crack propagation of B-03.

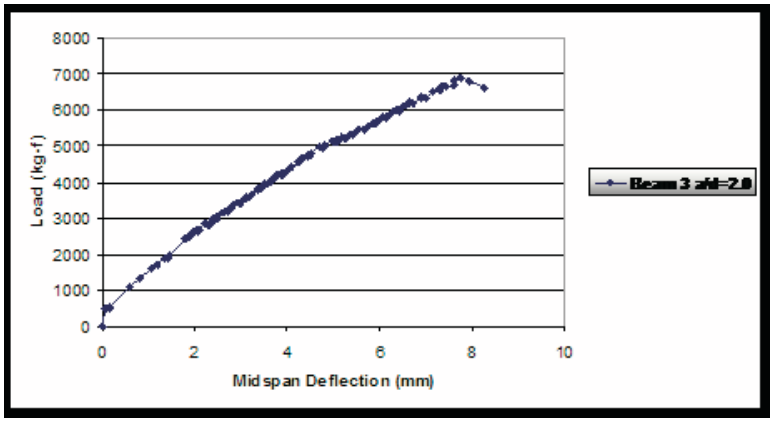

Figure 4.10. Load-Midspan deflection relationship for B-03.

Figure 4.11. Crack propagation of B-04.

Figure 4.12. Damaged shape of B-043.

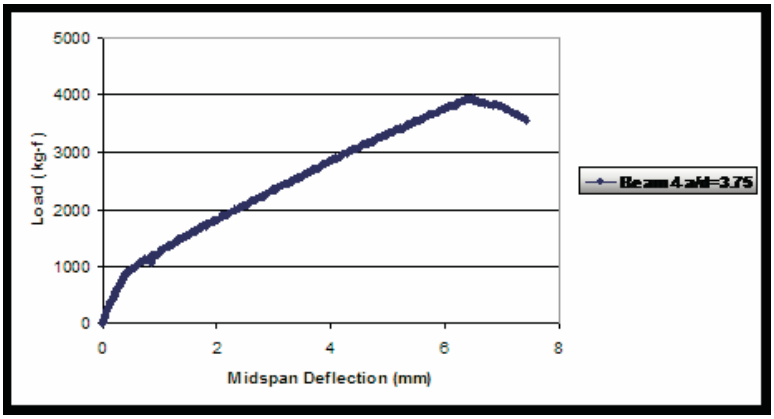

Figure 4.13. Load-Midspan deflection relationship for B-04.

Figure 4.14. Crack propagation of B-05.

observed as 1.32 MPa and 12.40 mm, respectively. Figure 4.16 shows load vs. mid-span deflection relation for B-05.

4.2.2.6. $B-06(V_f : 0.25\% + 0.50\%, a/d : 3.75)$:. This beam had the same failure mode known as diagonal tension failure with the beams which had a/d = 3.75 (B-02 and B-04). Ultimate and cracking stresses increased with an increase in fiber volume. The values for ultimate and cracking stresses were 1.66 MPa and 0.68 MPa, respectively. The midspan deflection was found as 7.86 mm. Figure 4.17, 4.18 and 4.19 illustrated crack propagation, damaged shape and load-midspan deflection curve for the B-06.

4.2.2.7. $B-07(V_f : 0.50\% + 0.50\%, a/d : 2)$:. The beam, had 1.0% fiber contents, had also same failure mode (shear compression) with other beams which had same a/d ratio. The different point was that failure was not sudden and brittle. First crack occurred in midspan. After first crack, inclined cracks developed. When the load was maximum point, shear compression failure occurred. The cracking and ultimate shear stresses were observed as 1.34 and 3.57 MPa. Figure 4.20 show crack propagation and damaged shaped of the specimen. Figure 4.22 showed the load-midspan deflection curve.

Figure 4.15. Damaged shape of B-05.

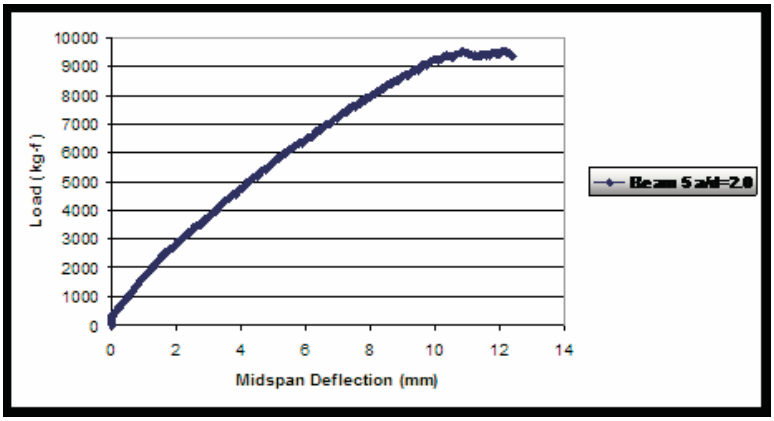

Figure 4.16. Load-Midspan deflection relationship for B-05.

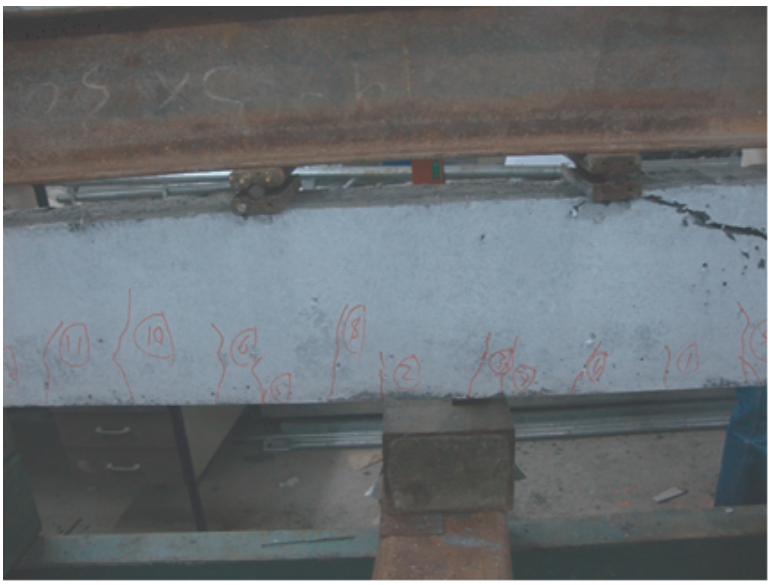

Figure 4.17. Crack propagation of B-06.

Figure 4.18. Damaged shape of B-06.

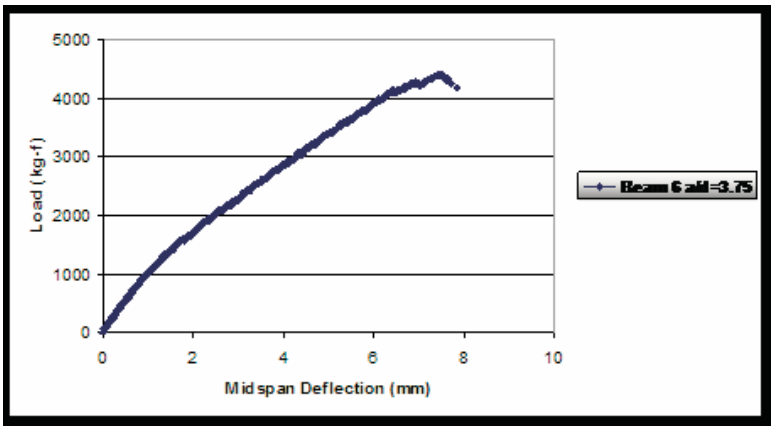

Figure 4.19. Load-Midspan deflection relationship for B-06.

Figure 4.20. Crack propagation of B-07.

Figure 4.21. Damaged shape of B-07.

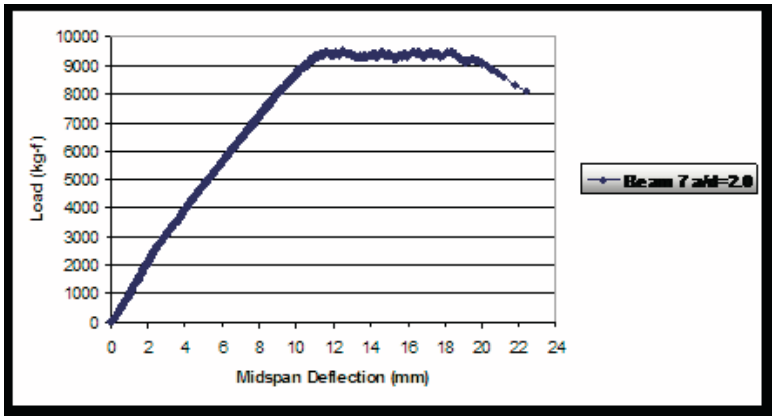

Figure 4.22. Load-Midspan deflection relationship for B-07.

Figure 4.23. Crack propagation and damaged shape of B-08.

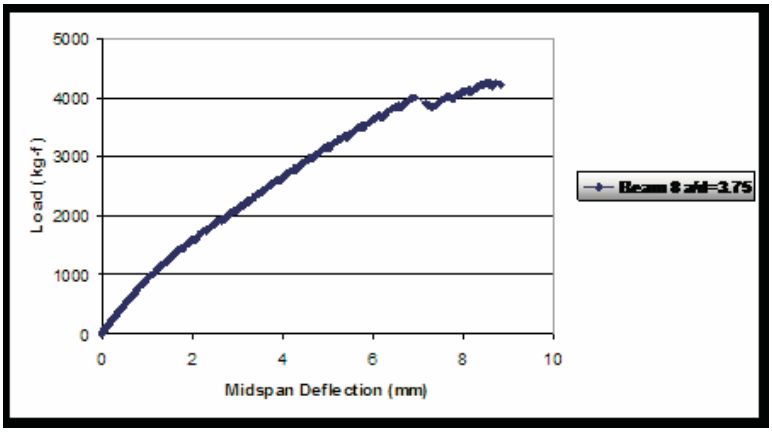

Figure 4.24. Load-Midspan deflection relationship for B-08.

4.2.2.8. $B-08(V_f : 0.50\% + 0.50\%, a/d : 3.75)$:. The failure is more brittle and sudden than $B-07$ because of high a/d ratio (3.75). The first crack was a flexural crack in the mid-span region. Flexural cracks increased after loading continued. After flexural cracks, inclined cracks formed in shear span region. Cracks in shear span expanded and continued to the load application point. Diagonal tension failure occurred finally. Cracking stress was 0.99 MPa and ultimate shear stress was 1.60 MPa. The maximum deflection in midspan was seen as 8.82 mm. Figures are shown below.

4.2.2.9. $B-09(V_f : 0.75\% + 0.75\%, a/d : 2)$:. The beam had maximum fiber content (1.50%). Failure mode was shear compression. The cracking stress was 1.52 MPa; the

Figure 4.25. Crack propagation of B-09.

ultimate shear stress was 3.70 MPa (maximum of those beams). Midspan deflection was observed as 13.67 mm. Figure 4.25 show the crack propagation and damaged shape of the beam.

4.2.2.10. $B-10(V_f : 0.75\% + 0.75\%, a/d : 3.75)$:. $B-10$ also had 1.50% fiber content and a/d ratio was 3.75. In this beam, diagonal tension failure occurred. The cracking stress was found as 1.11 MPa, the ultimate shear stress was calculated as 2.05 MPa (maximum of those beams which had a/d=3.75). Midspan deflection was observed as 13.49mm. This beam behaved more ductile than others (had a/d=3.75). Figure 4.28 show the crack propagation and damaged shape of the beam. Figure 4.30 illustrates load-midspan deflection curve.

Table 4.2 shows the results of tests. In the table; shear span-to-effective depth ratio (a/d), volume fraction (%), compressive strength (f_{ck}), average density of the cylinder specimen (g/cm^3), cracking stress ($V_{cr}/b_w d$), ultimate shear stress ($V_u/b_w d$), normalized shear stress ($V_{max}/\sqrt{f_c} b_w d$), maximum midspan deflection (mm) and failure mode of the beams are indicated.

Figure 4.26. Damaged shape of B-09.

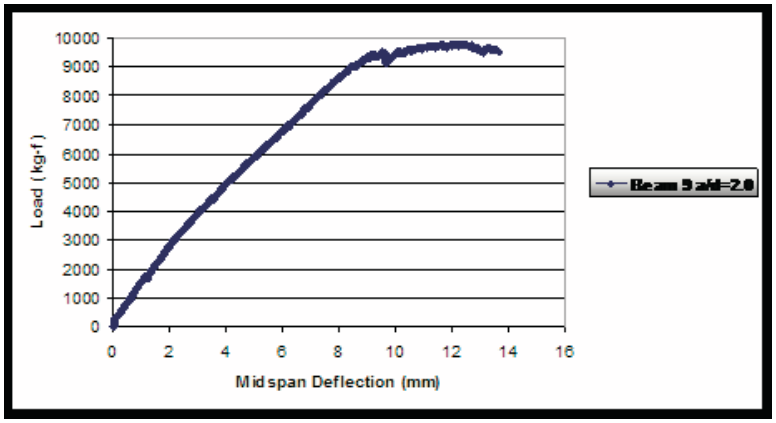

Figure 4.27. Load-Midspan deflection relationship for B-09.

Figure 4.28. Crack propagation of B-10.

Figure 4.29. Damaged shape of B-10.

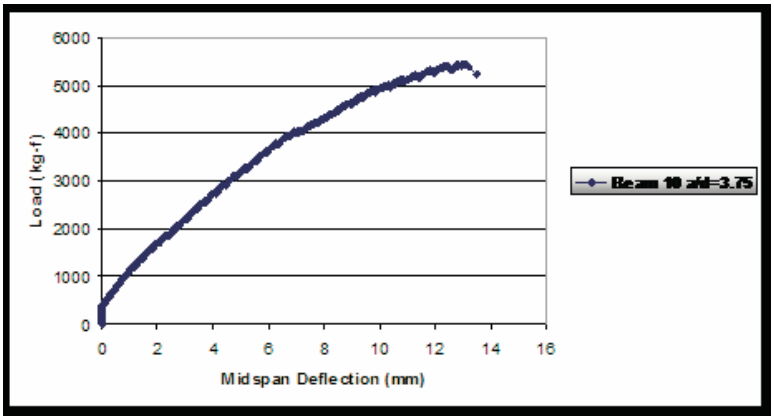

Figure 4.30. Load-Midspan deflection relationships for B-10.

Table 4.2. Summary of experimental results.

Specimen	a/d	Volume Fraction ($V_f, \%$)	F_{ck} (MPa)	Average Density of the Cylinder Specimen (g/cm^3)	$V_{cr}/b_w d$ (MPA)	$V_u/$ $b_w d$ (MPA)	V_{max} $/\sqrt{f_c} b_w d$	Maximum Midspan Deflection (mm)	Failure Mode
B-01	2.00	0.00	59.27	2.44	1.08	2.62	0.34	8.90	Shear-Compression
B-02	3.75	0.00	59.27		0.52	1.32	0.17	6.10	Diagonal Tension
B-03	2.00	0.25 + 0.25	39.11	2.20	1.08	2.60	0.42	8.25	Shear-Compression
B-04	3.75	0.25 + 0.25	39.11		0.42	1.49	0.24	7.43	Diagonal Tension
B-05	2.00	0.25 + 0.50	39.51	2.14	1.32	3.60	0.57	12.40	Shear-Compression
B-06	3.75	0.25 + 0.50	39.51		0.68	1.66	0.26	7.86	Diagonal Tension
B-07	2.00	0.50 + 0.50	39.58	2.15	1.34	3.57	0.57	22.42	Shear-Compression
B-08	3.75	0.50 + 0.50	39.58		0.99	1.60	0.25	8.82	Diagonal Tension
B-09	2.00	0.75 + 0.75	38.71	2.19	1.52	3.70	0.59	13.67	Shear-Compression
B-10	3.75	0.75 + 0.75	38.71		1.11	2.05	0.33	13.49	Diagonal Tension

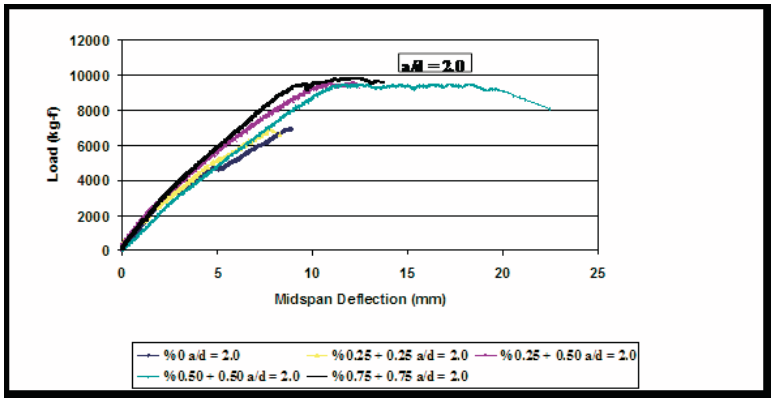

Figure 4.31. Load-Midspan Deflection Curves at a/d = 2.0.

4.3. Discussion of Experimental Results

In this part of the thesis, first the performances of beams with different hybrid fiber volume ratios were compared. Then, the results of this thesis were evaluated together with another study made by using non hybrid fibers (Şen, 2009).

4.3.0.11. Effect of Shear Span-to-Effective Depth Ratio (Table 4.2). All beams with a/d = 2 had shear-compression failure as expected. The failure was brittle and sudden except the Beam 07. Ultimate average shear stress ($V_u/b_w d$) increased with an increased amount of fibers. Most pronounced increase was seen when the fiber amount is increased from 0.5% to 0.75%. For fiber volume ratios between $0.75 - 1.5\%$, the increase in shear capacity ($V_u/b_w d : 3.60 - 3.70$, $V_{max}/\sqrt{f_c} b_w d : 0.57 - 0.59$) was not found to be pronounced. A similar result is seen when first cracking stress values were examined. First cracking stress was increased with an increasing fiber volume. The most pronounced increments were observed when the fiber volume increased from 0.5% to 1.00%. Load-mid span deflections for these beams are given in Figure 4.31. As is seen in the figure, mid span deflections were increased with an increase in fiber volume ratio. An important result is that the failure mode was not affected when fiber volume ratio was increased.

All beams with a/d = 3.75 had diagonal tension failure. The failure was brittle and sudden. Ultimate shear stress ($V_u/b_w d$) increased with an increased amount of

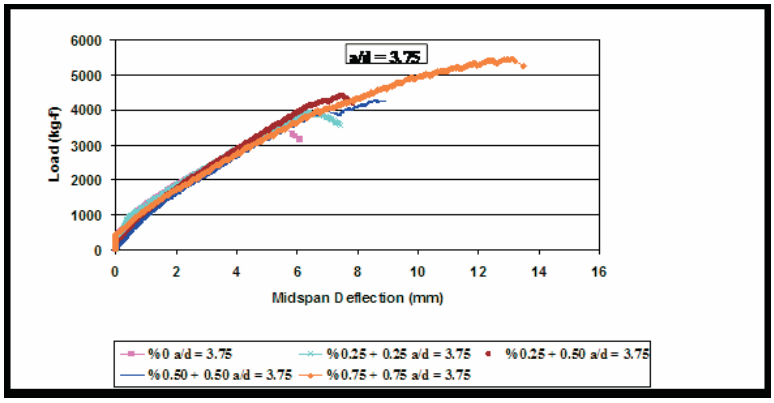

Figure 4.32. Load-Midspan Deflection Curves at a/d = 3.75.

fibers. Most pronounced increase was seen when the fiber amount is increased from 0% to 0.50%. This is different from the result mentioned above (a/d= 2). For fiber volume ratios between 0.50 - 1.00%, the increment in shear capacity ($V_u/b_w d$: $1.49 - 1.66$, $V_{max}/\sqrt{f_c} b_w d$: $0.24 - 0.26$) was not found to be pronounced. A similar result is seen when first cracking stress values were examined. First cracking stress was increased with an increasing fiber volume. The most noticeable increments were observed when the fiber volume increased from 0.5% to 0.75% and from 1.00% to 1.5%. Load-mid span deflections for these beams are given in Figure 4.32. As is seen in the figure, mid span deflections were found to increase when compared to plain concrete as expected. However, the increment in midspan deflection was noticeable only when high volumes of fibers were used (1.5%). As mentioned above, failure mode was not affected when fiber volume was increased.

Figure 4.33 compares load-mid span deflections for the two a/d ratios studied. As can be seen from the figures almost all of the beams (except for 0.5%) with an a/d of 2 showed strain-hardening due to fibers. This behavior was not seen when a/d is 3.75 (except when high volumes of fibers were used). This means that fibers role is more important when a/d is 2 (when the failure mode is shear compression). This phenomenon will be explained in detail later in section 4.4.

Figure 4.34 shows variation of normalized shear stress with an increasing fiber volume ratio and shear span to effective depth ratio. As is seen from the figure shear capacity increased with increasing fiber volume ratio. Only exception to this is seen

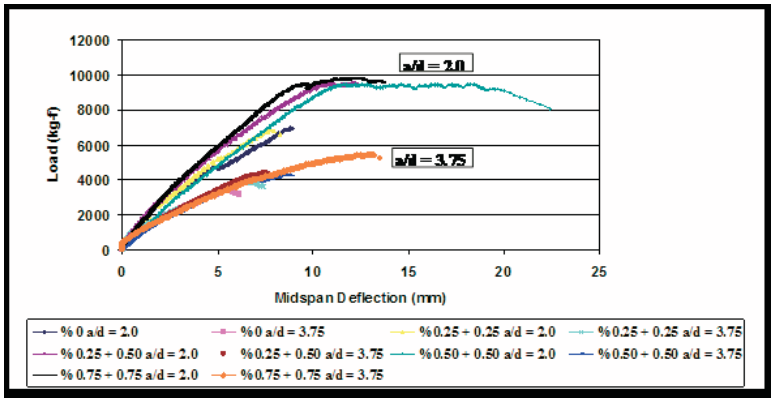

Figure 4.33. Load-Midspan Deflection Curves at a/d = 2.0 and 3.75.

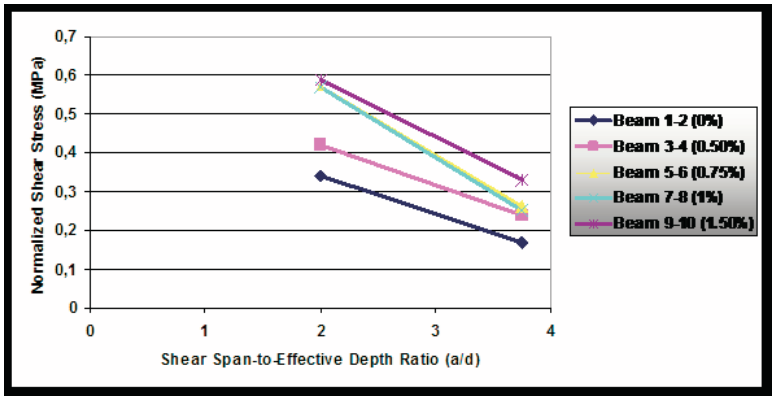

Figure 4.34. $V_{max}/\sqrt{f_c}b_w d$ relations with Shear Span-to-Effective Depth Ratio.

when fiber volume ratio was increased from 0.75 to 1.00%. This result is consistent with the result obtained from small-size specimens. Load vs. crack opening curves of the small size specimens had been found very similar for increasing fiber volume ratio (Figure 4.34). Shear capacity decreased when a/d ratio was increased as expected

Figure 4.35 shows the effect of increased fiber volume for different a/d ratios. Effect of fibers are very well seen when fiber volume ratio was increased from 0 to 0.5 and 0.75%. Over 0.75%, fibers' affect is less pronounced. This result agrees well with the results obtained from the small size beams (Section 4.2.1.2). Contribution of fibers to bending load had been found similar for fiber volume ratios greater than 0.75%.

In the next figure, increase in percentage of shear capacity of concrete for various fiber contents is given. Important contribution of fibers is seen for all fiber volumes.

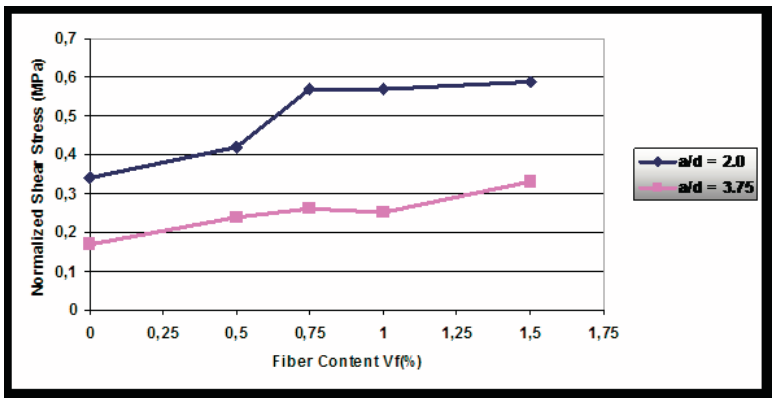

Figure 4.35. Effect of fiber content.

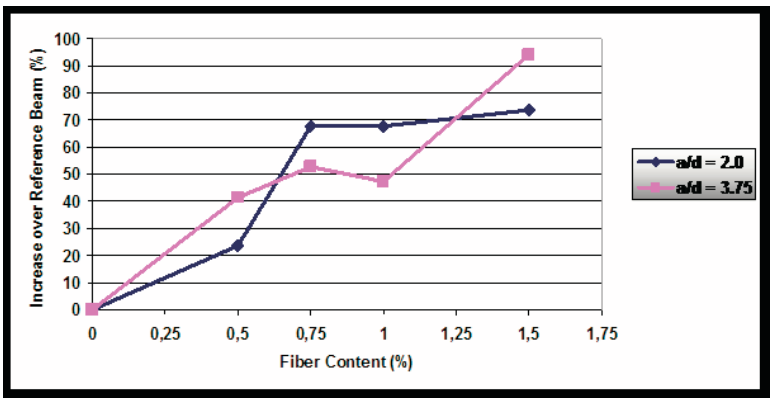

Figure 4.36. The relationship between increase over Reference Beam and Fiber Content.

4.4. Comparison of the test results with the previous study (Şen, 2009)

The results of this study were compared with the results of a similar study carried out in Bogaziçi University as mentioned above. The results obtained by using similar size beams are given in Table 4.3. In this previous study, one type of fiber was used for all beams, maximum fiber volume was 0.75% and concrete strength was approximately 60 MPa for all the beams. The results of (Şen, 2009) were compared with the current study.

Table 4.3. Summary of experimental results of a previous study (experimental procedures, specimen dimensions are the same, compressive strength of concrete, and fiber volume ratios are different) (Şen, 2009).

Specimen	a/d	Concrete Type	Volume Fraction (V_f, %)	Aspect Ratio L/D	f_{ck} (MPa)	V_{cr} $/b_w d$ (MPa)	V_u $/b_w d$ (MPa)	V_{max} $\sqrt{f_c}/$ $b_w d$	Midspan Deflection (mm)	Failure Mode
BEAM-01	2.00	HSC	0.00	-	57.57	1.13	2.56	0.34	12.4	Shear Comp.
BEAM-02	3.75	HSC	0.00	-	57.57	0.78	1.27	0.17	6.62	Diagonal Tension
BEAM-03	2.00	HSC	0.50	65	60.16	1.25	2.73	0.35	12.80	Shear Comp.
BEAM-04	3.75	HSC	0.50	65	60.16	0.97	1.56	0.20	10.38	Diagonal Tension
BEAM-05	2.00	HSC	0.75	65	61.68	1.42	2.94	0.37	13.28	Shear Comp.
BEAM-06	3.75	HSC	0.75	65	61.68	1.09	1.74	0.22	60.50	Flexure
BEAM-07	2.00	HSC	0.50	80	60.86	1.34	2.94	0.38	13.40	Shear Comp.
BEAM-08	3.75	HSC	0.50	80	60.86	0.89	1.39	0.18	12.80	Diagonal Tension
BEAM-09	2.00	HSC	0.75	80	63.59	1.58	3.38	0.42	57.34	Flexure
BEAM-10	3.75	HSC	0.75	80	63.59	1.18	1.80	0.23	63.80	Flexure

The authors used the same fibers (65/35 and 80/60) as in this study, however they did not use hybrid combination of the fibers. Instead they put only one type of fiber to each beam. When Table 4.3 (Şen, 2009) is examined, it is seen that shear compression failure was seen for a/d of 2 except for one specimen (BEAM-09). The ultimate shear capacity and the normalized shear stress values were found to increase when the fiber volume ratio was increased from 0 to 0.75% (BEAM-01, BEAM-03, and BEAM-05). The results of the two studies were compared in the (Table 4.4 and 4.5).

Table 4.4. Comparison of test results of current and previous study (Şen, 2009) for a/d = 2.00.

Volume Fraction (%)		Compressive Strength f_c (MPa)		Aspect Ratio (L/D)	$(V_{max}/\sqrt{f_c}b_w d)$	Normalized Shear Stress	
Current Study	Previous Study	Current Study	Previous Study	Current Study	Previous Study	Current Study	Previous Study
0	0	59.27	57.57	-	-	0.34	0.34
0.25 + 0.25	0.50	39.11	60.16	65 + 80	65	0.42	0.35
0.25 + 0.50	0.75	39.51	61.68	65 + 80	65	0.57	0.37
0.25 + 0.25	0.50	39.11	60.86	65 + 80	80	0.42	0.38
0.25 + 0.50	0.75	39.51	63.59	65 + 80	80	0.57	0.42

Table 4.5. Comparison of test results between current and previous study (Şen, 2009) for a/d = 3.75.

Volume Fraction (%)		Compressive Strength f_c (MPa)		Aspect Ratio (L/D)	$(V_{max}/\sqrt{f_c}b_w d)$	Normalized Shear Stress	
Current Study	Previous Study	Current Study	Previous Study	Current Study	Previous Study	Current Study	Previous Study
0	0	59.27	57.57	-	-	0.17	0.17
0.25 + 0.25	0.50	39.11	60.16	65 + 80	65	0.24	0.20
0.25 + 0.50	0.75	39.51	61.68	65 + 80	65	0.26	0.22
0.25 + 0.25	0.50	39.11	60.86	65 + 80	80	0.24	0.18
0.25 + 0.50	0.75	39.51	63.59	65 + 80	80	0.26	0.23

As can be seen from the tables normalized shear stress values were compared to exclude the effect of compressive strength. The beams with hybrid fiber combinations showed higher shear stress for all fiber volume ratios for both shear span-to-effective depth ratios. However, the effect of using hybrid fiber combination was more noticeable for a/d of 2.00. This is most probably due to different failure patterns of the beams with different a/d ratios. When a/d ratio is 2.0, all the beams showed shear compression type of failure. In this type of failure crack opening before failure of the beam is found to be large. Hence, during this type of failure fibers responsibility for bearing load is also high. On the other hand, when a/d is 3.75, a narrower but longer crack leads the specimens to failure. To mathematically express this result, crack openings were measured for all the beams from the pictures taken during the experiments (crack lengths were calculated by using AUTOCAD from the known value of specimen size). Calculations were made for 3 points for each beam and average of the three values was used. Average crack opening was found to vary between 1.45 - 2.92 cm when a/d is 2.00 while it changed between 0.90 - 1.15 cm when a/d is 3.75. Therefore fibers contribution to load bearing may be less for large a/d when compared to the specimens with smaller a/d ratios. From this result it can be concluded that fibers role is more important when shear compression type of failure occurs.

Comparison of the current and previous study (Şen, 2009) are made according to normalized shear stress vs. shear span-to-effective depth ratio (Figure 4.37 and 4.38), normalized shear stress vs. fiber contents (Figure 4.39) and increase over reference beam vs. fiber contents (Figure 4.40). Effect of hybrid fibers is very well seen in the figure when fiber volume ratio was increased from 0 to 0.5 and 0.75% at a/d= 2.0. Effect of using hybrid fibers is again seen when a/d ratio is large (3.75). However this time the increment is less pronounced due to the reasons explained above (Section 4.4).

As can be seen from the Figure 4.39 normalized shear stress values increase with an increase in fiber content (from 0% to 0.75%) for all the beams. A similar trend was observed for all the beams. Only exception was seen when fiber volume ratio was increased from 0.5 to 0.75% for the hybrid fiber reinforced beams with an a/d of 2.00. Fibers were found to be more effective for this specimen. This result agrees well with

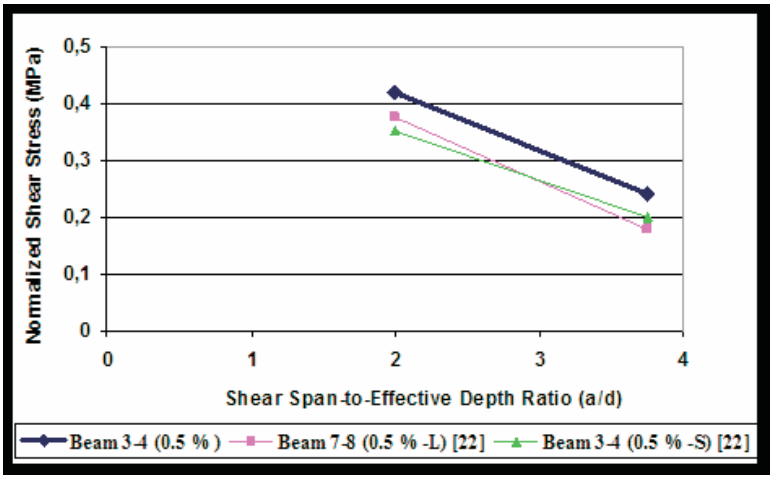

Figure 4.37. $V_{max}/\sqrt{f_c}b_w d$ relations with Shear Span-to-Effective Depth Ratio for 0.5% Fiber Content (Current and (Şen, 2009).

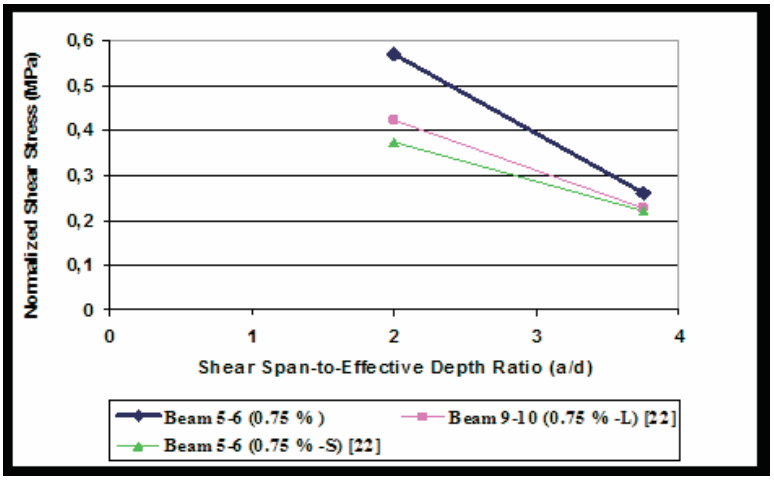

Figure 4.38. $V_{max}/\sqrt{f_c}b_w d$ relations with Shear Span-to-Effective Depth Ratio for 0.75% Fiber Content (Current and (Şen, 2009)).

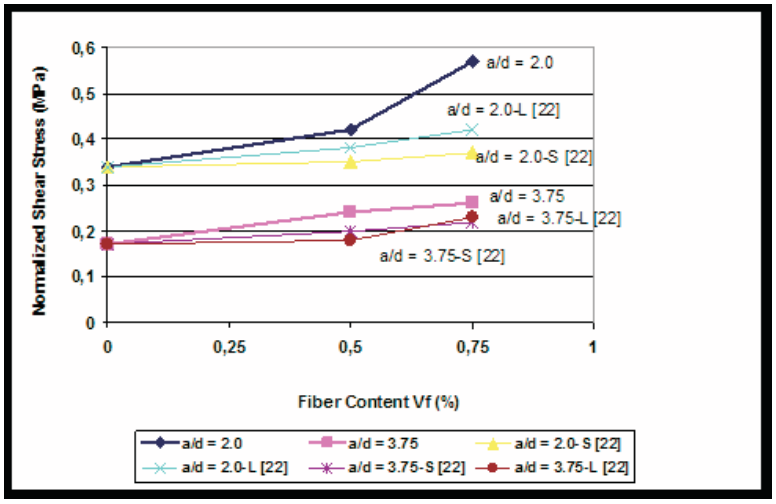

Figure 4.39. The relationship between $V_{max}/\sqrt{f_c}b_w d$ and Fiber Content (Current vs. (Şen, 2009)).

the previous results given above (Section 4.4). Since crack opening is greater when a/d is small, using larger volumes of hybrid fibers becomes more important. Short fibers arrest small cracks, while longer fibers arrest and hold larger cracks. Higher energy absorption is then made possible, leading to a greater ductility.

In Figure 4.40, percent increase in shear capacity increases with an increase in fiber content according to reference beam (plain concrete) was given. Most noticeable increase (approximately 45%) was seen in the current study when the fiber content is increased from 0.50 to 0.75% at a/d=2.0. In the previous study (Şen, 2009), most pronounced increase was seen when the fiber content is increased from 0.50% to 0.75% also. From these results it can be concluded that important improvements in shear capacity over reference beams can be obtained by using fibers.

4.5. Comparison of the test results with the previous studies

The wide study on the shear behavior of reinforced concrete beams with and without fibres indicates that the nominal stress at shear cracking and the ultimate shear strength increase with decreasing shear span-to-effective depth ratio and increasing concrete compressive strength, longitudinal reinforcement ratio, and fibre volume fraction. These experimental studies demonstrated that steel fibres have significant

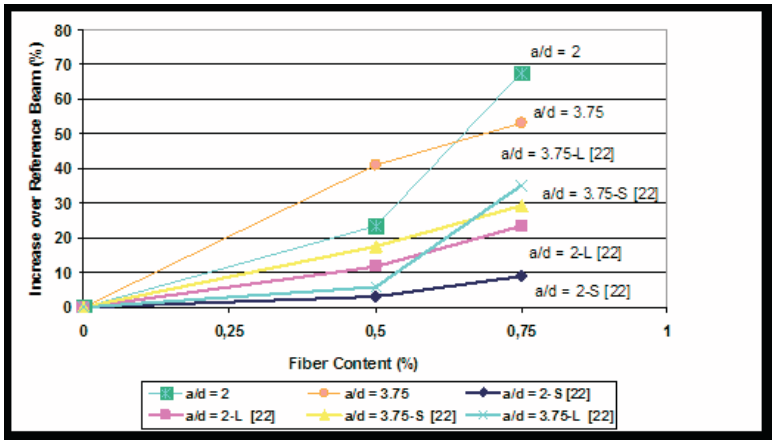

Figure 4.40. The relationship between increase over Reference Beam and Fiber Content (Current vs. (Şen, 2009)).

influence on shear resistance. It is recommended in the studies that steel fibres can replace the conventional web reinforcement in beams (Şen, 2009).

According to the study made by Sydney Furlan Jr. et al., fiber volume fraction was used 0 to 2%. The main alterations resulting from the use of fibers were increased shear strength, stiffness (particularly after first crack stage) and ductility. In the current study, shear strength and first crack strength also increased with an increase of hybrid fiber volume.

Another study made by Madan et al., three different steel fiber volume fractions were used. The test results indicate that the fibers have significant influence on the shear strength of a longitudinally reinforced concrete beams. Shear strength increases with increasing fiber volume and decreasing shear span-to-effective depth ratio. This information is convenient with the current study as expected.

5. CONCLUSIONS

The main objective of this study was to investigate the effects of hybrid fibers on shear capacity of large size reinforced concrete beams. Ten hybrid fiber reinforced beams were cast. Fiber volume was increased up to 1.5%. Two fibers with different lengths (35 mm and 65 mm) were used for hybrid combinations. Four-point bending tests were applied. Effects of shear span to effective depth ratio, fiber volume, hybrid combination on mechanical performance were discussed. In addition to that, results of this study was compared with the results of a previous study (Şen, 2009) in order to observe the differences between hybrid and one type of fiber reinforced concrete performances.

Shear span to effective depth ratio; 2 shear span to effective depth ratios were chosen, 2.0 and 3.75. All the beams with an a/d of 2.00 showed shear compression type of failure. On the other hand, the beams with an a/d of 3.75 showed diagonal tension type of failure as expected. First crack stress and ultimate shear stress were found to decrease when shear span-to-effective depth ratio increased. These results were consistent with previous study (Şen, 2009) and literature. Failure mode was seemed to not change with increasing fiber volume ratio. From here it can be resulted that a/d value is the main parameter affecting failure mode.

Fiber volume ratio; shear capacity of the beams were found to increase with an increase in fiber volume ratio. The greatest increase was observed when fiber volume ratio was increased from 0.5 to 0.75%. Increments were also observed when fiber volume ratio was increased to 1.0% and 1.5%. However the increase in shear capacity was more pronounced for small fiber volume ratios. Fiber contribution was found to vary for different failure modes. Fiber contribution was higher when a/d ratio was small. This could be explained as follows: for an a/d ratio of 2, shear compression type of failure was seen and opening of main crack before failure of beam was relatively high (change from 1.45 to 2.92 cm) when compared to a/d of 3.75 (change from 0.90 to 1.15 cm) Therefore, fibers play a more important role when crack opening is high (a/d is

2). When a/d is 3.75, opening of crack before failure is much smaller and fibers' role is relatively small. Effect of using fibers was also seen when small size beams were tested. These specimens (without rebars) were tested to see the effect of fibers on concrete alone. Transition from strain softening to strain hardening is seen when fiber volume increased to 0.75% and the specimens with higher fiber volume ratios (1.00% and 1.5%) show strain hardening behavior. This means greater energy absorption during failure. These results are consistent with the results obtained from large-size specimens.

Comparison of hybrid fiber and single fiber reinforced beams: the results of this study were compared with the results of a previous study. Similar size beams and similar experimental set-ups were used for comparative purposes. Both study used steel fibers. Previous study uses short and long steel fibers separately. In this study short and long steel fibers were combined together to see the effects of using hybrid fibers. Concrete strength of the beams cast were found to be different (previous study yielded relatively higher results for fiber reinforced beams) for the two study. Therefore, normalized shear stress values ($_{max}$ / $\sqrt{f_c}b_w d$) were calculated to exclude the effect of compressive strength when comparing the results of previous study (Şen, 2009) and the current study. Following results were drawn as a result of comparison: a) shear capacity of hybrid fiber reinforced concretes were found to be higher than the shear capacity of the single fiber reinforced beams. This is probably due to effective crack arresting mechanism of hybrid fibers. Short fibers arrest small size cracks and long fibers arrest large size cracks and crack opening is delayed due to this mechanism. b) Increase in shear capacity due to decreased a/d (2.0) was found to be more pronounced when hybrid combinations were used. Since fibers' role was found to be more important when shear compression type of failure under consideration (when a/d is 2). Then, explanation of having greater increase in shear capacity when a/d is small for current study can be made considering the effect of hybrid fiber mechanism.

REFERENCES

Arslan, G., 2008 *Cracking Shear Strength of RC Slender Beams without Stirrups*, Journal of Civil Engineering and Management, Istanbul, Turkey.

Ersoy, U., 1994 *Reinforced Concrete*, Text Book, Middle East Technical University, Turkey.

Chanh, N. V., 2005, *Steel Fiber Reinforced Concrete*, Faculty of Civil Engineering, Ho Chi Minh City University of Technology.

Shah, S.P. and Batson, G.B. 1987, Fiber Reinforced Concrete: Properties and Applications, $http://en.wikipedia.org/wiki/Fibre-reinforcedconcrete$, April 2010.

Greenough, T. and M. Nehdi, 2008, *Shear behavior of Fiber-Reinforced Self-Consolidating Concrete Slender Beams*, ACI Material Journals, Canada.

Imam, M. Et al., 1997, *Shear domain of fibre-reinforced high-strength concrete beams*, Engineering Structures, Volume 19, Number 9, pp. 738-747.

Lim, D. H., 1999, *Experimental and theoretical investigation on the shear of steel fibre reinforced concrete beams*, Engineering Structures, Volume 21, pp. 937-944.

Lofgren, I., 2005, *Fibre-reinforced Concrete for Industrial Construction*, Ph.D. Thesis, Department of Civil and Environmental Engineering, Chalmers University of Technology, Sweden.

Kutzing, L. 1997, *Shear Strength of Steel Fibre Reinforced Concrete Beams and Plates*, Technical Report, University of Leipzig, Germany.

Madan, S. K., Kumar, G. R. and S. P. Singh, 2007 *Steel Fibres as Replacement of Web Reinforcement for RCC Deep Beams in Shear*, Technical Report, India.

Majdzadeh, F., Soleimani, S. M. and N. Banthia, 2006, *Shear strength of reinforced concrete beams with a fiber concrete matrix*, Canadian Journal of Civil Engineering, Volume 33, Number 6, pp. 726-734.

Mansur, M. A. et al., 1986 *Shear Strength of Fibrous Concrete Beams Without Stirrups*, Journal of Structural Engineering, Volume 112, Number 9.

Narayanan, R. and Y. S. Darwish, 1987, *Use of Steel Fibers as Shear Reinforcement*, ACI Structural Journal.

Junior, S. F. and J. B. de Hanai, 1997, *Shear Behaviour of Fiber Reinforced Concrete Beams*, Cement and Concrete Composites, Volume 19, pp. 359-366.

Oh, J. K. and S. W. Shin, 2001 *Shear Strength of Reinforced High-Strength Concrete Deep Beams*, ACI Structural Journals, Volume 98, Number 2, pp.164-173.

Steel fibre reinforced concrete (SFRC) - Quality, performance and specification BOSFA.

Şen, M., 2009, *Shear Behavior of Frc Beams Without Web Reinforcement Using Steel fibres With Different Aspect Ratios*, M.S. Thesis, Department of Civil Engineering, Bogaziçi University.

TS-500, 2007 *Betonarme Yapıların Hesap ve Yapım Kuralları*, Turkish Standards.

Wang, C. and C. G. Salmon,1979, *Reinforced Concrete Design*, Text Book, Longman Higher Education, University of Wisconsin, USA.

Mishra, G., 2009, Steel Fibre Reinfoced Concrete, $http://theconstructor.org/concrete/steel-fibre-reinforced-concrete/4771$.

Yang, K. H. et al., 2003 *Shear Characteristics of high-strength concrete deep beams without shear reinforcements*, Engineering Structures, pp. 1343-1352, 2003.

Yerlikaya, M. 2005, *Çelik Tel Donatılı Zemin Betonları Tasarım ve Yapım İlkeleri*

BEKSA Çeliktel1.pdf.